AMERICAN SOCIETY FOR MICROBIOLOGY | Applied and Environmental Microbiology®

GENETICS AND MOLECULAR BIOLOGY

Heat Shock Repressor HspR Directly Controls Avermectin Production, Morphological Development, and H_2O_2 Stress Response in *Streptomyces avermitilis*

Xiaorui Lu,[a] Qian Wang,[a] Mengyao Yang,[a] Zhi Chen,[a] Jilun Li,[a] Ying Wen[a]

[a]State Key Laboratory of Agrobiotechnology and College of Biological Sciences, China Agricultural University, Beijing, China

Xiaorui Lu and Qian Wang contributed equally to this work. Author order was determined by drawing straws.

ABSTRACT The heat shock response (HSR) is a universal cellular response that promotes survival following temperature increase. In filamentous *Streptomyces*, which accounts for ~70% of commercial antibiotic production, HSR is regulated by transcriptional repressors; in particular, the widespread MerR-family regulator HspR has been identified as a key repressor. However, functions of HspR in other biological processes are unknown. The present study demonstrates that HspR pleiotropically controls avermectin production, morphological development, and heat shock and H_2O_2 stress responses in the industrially important species *Streptomyces avermitilis*. HspR directly activated *ave* structural genes (*aveA1* and *aveA2*) and H_2O_2 stress-related genes (*katA1*, *catR*, *katA3*, *oxyR*, *ahpC*, and *ahpD*), whereas it directly repressed heat shock genes (HSGs) (the *dnaK1-grpE1-dnaJ1-hspR* operon, *clpB1p*, *clpB2p*, and *lonAp*) and developmental genes (*wblB*, *ssgY*, and *ftsH*). HspR interacted with PhoP (response regulator of the widespread PhoPR two-component system) at *dnaK1p* to corepress the important *dnaK1-grpE1-dnaJ1-hspR* operon. PhoP exclusively repressed target HSGs (*htpG*, *hsp18_1*, and *hsp18_2*) different from those of HspR (*clpB1p*, *clpB2p*, and *lonAp*). A consensus HspR-binding site, 5′-TTGANBBNNHNNNDSTSHN-3′, was identified within HspR target promoter regions, allowing prediction of the HspR regulon involved in broad cellular functions. Taken together, our findings demonstrate a key role of HspR in the coordination of a variety of important biological processes in *Streptomyces* species.

IMPORTANCE Our findings are significant to clarify the molecular mechanisms underlying HspR function in *Streptomyces* antibiotic production, development, and H_2O_2 stress responses through direct control of its target genes associated with these biological processes. HspR homologs described to date function as transcriptional repressors but not as activators. The results of the present study demonstrate that HspR acts as a dual repressor/activator. PhoP cross talks with HspR at *dnaK1p* to coregulate the heat shock response (HSR), but it also has its own specific target heat shock genes (HSGs). The novel role of PhoP in the HSR further demonstrates the importance of this regulator in *Streptomyces*. Overexpression of *hspR* strongly enhanced avermectin production in *Streptomyces avermitilis* wild-type and industrial strains. These findings provide new insights into the regulatory roles and mechanisms of HspR and PhoP and facilitate methods for antibiotic overproduction in *Streptomyces* species.

KEYWORDS HspR, *Streptomyces avermitilis*, avermectin, morphological development, heat shock response

Streptomyces species are Gram-positive, filamentous soil bacteria that undergo complex morphological development involving the formation of substrate hyphae, aerial hyphae, and spore-bearing hyphae (1). They are an economically important group

Citation Lu X, Wang Q, Yang M, Chen Z, Li J, Wen Y. 2021. Heat shock repressor HspR directly controls avermectin production, morphological development, and H_2O_2 stress response in *Streptomyces avermitilis*. Appl Environ Microbiol 87:e00473-21. https://doi.org/10.1128/AEM.00473-21.

Editor Maia Kivisaar, University of Tartu

Address correspondence to Ying Wen, wen@cau.edu.cn.

Received 9 March 2021
Accepted 12 June 2021
Accepted manuscript posted online 23 June 2021
Published 11 August 2021

that produce a wide variety of secondary metabolites, notably, antibiotics having antibacterial, antifungal, antiviral, anthelmintic, anticancer, or immunosuppressive activity (2, 3). Antibiotic biosynthesis is generally associated with development and controlled by multiple levels of transcriptional regulators (TRs), including cluster-situated regulators (CSRs) and higher-level pleiotropic/global regulators, in response to environmental and physiological cues such as low nutrient availability, temperature changes, and pH changes (4–6).

All cellular organisms respond to sudden temperature increases by substantially raising levels of heat shock proteins (HSPs). HSPs are divided into two major classes: (i) molecular chaperones that promote correct folding of denatured and newly synthesized proteins and prevent formation of insoluble protein aggregates (e.g., DnaK, DnaJ, GrpE, GroES, and GroEL), and (ii) ATP-dependent proteases involved in the degradation of denatured proteins (e.g., ClpAP, ClpXP, ClpB, and Lon) (7–9). These HSPs are essential for normal cell growth and are synthesized at a basal level under physiological conditions. Induction of HSPs under stress conditions (particularly heat shock) is a universal response, but synthesis of HSPs is controlled by a variety of mechanisms depending on the bacterial species. In *Escherichia coli*, two alternative sigma factors, Sig32 and SigE, activate heat shock genes (HSGs) in response to denatured proteins generated in cytoplasm (Sig32) or periplasm (SigE) following stimulation (10). In *Streptomyces*, HSGs are mainly negatively regulated by three repressors: HrcA, RheA, and HspR (10). HrcA in *Streptomyces albus* represses *hrcA-dnaJ2*, *groES-groEL1*, and *groEL2* operons (11). The RheA regulon of *S. albus* consists of its own gene *rheA* and nearby divergently transcribed gene *hsp18* (12). The HspR repressor is a member of the MerR-family TRs that contain conserved helix-turn-helix (HTH) DNA-binding motif at the N terminus and function as homodimers. HspR represses the *dnaK-grpE-dnaJ-hspR* operon and *clpB* and *lon* genes by interacting with HspR-binding site HAIR (HspR-associated inverted repeat [5′-TTGAGY-N_7-ACTCAA-3′]) at target promoter regions in *Streptomyces coelicolor*, *S. albus*, and *Streptomyces lividans* (13–17). The *S. coelicolor* DnaK chaperone functions as a corepressor of the HspR regulon by binding to HspR at HAIR sites (14, 18). HspR itself can bind DNA targets, but formation of a stable complex with the DNA targets requires HspR-DnaK interaction. During heat shock, DnaK is titrated by denatured proteins and unable to bind to HspR, leading to the induction of target HSGs (14, 18). The reported studies have only addressed the role of *Streptomyces* HspR in the heat shock response (HSR), and nothing is known regarding its role in *Streptomyces* development and antibiotic production.

HspR is present in other actinomycetes besides *Streptomyces*, including *Mycobacterium tuberculosis* (19). HSPs contribute to *M. tuberculosis* virulence and are induced following entry into host cells to protect *M. tuberculosis* against stress imposed by host macrophages. Among *M. tuberculosis* HSPs, Acr2 is a member of the α-crystallin family of molecular chaperones and plays a key role during the *M. tuberculosis* stress response. HspR functions as a repressor of *acr2* expression (19). Another *acr2* repressor, PhoP, the response regulator of the widespread PhoPR two-component system, interacts with HspR at the *acr2* promoter region to coregulate *acr2* expression (20). PhoP is not necessary for the DNA-binding activity of HspR; however, HspR-PhoP interaction stabilizes the higher-order DNA-protein complex to prevent access of RNA polymerase to the *acr2* promoter, thus repressing the initiation of transcription. *M. tuberculosis dnaK* is repressed by HspR (19) but is not regulated by HspR-PhoP interactions (20).

The PhoPR two-component system, which senses and responds to phosphate limitation stress, is well conserved in *Streptomyces*. PhoP acts as a master regulator for the coordination of a variety of physiological processes, including phosphate metabolism, nitrogen metabolism, respiration, development, and antibiotic biosynthesis (21–24). PhoP cross talks with GlnR (main nitrogen metabolism regulator) and AfsR (response regulator of AfsRK two-component system that promotes antibiotic biosynthesis in *S. coelicolor*) by competing for binding to the same target promoter regions in control of

nitrogen metabolism and antibiotic biosynthesis (25, 26). A role of PhoP in HSR and its cross talk with other regulators in *Streptomyces* has not been reported.

The industrial species *Streptomyces avermitilis* produces avermectins, a series of 16-membered macrocyclic anthelmintic antibiotics that are widely used in agricultural and medical fields and have great commercial importance (27, 28). The heat shock repressor HspR has not yet been studied in *S. avermitilis*. The role of HspR in antibiotic production and development in this species is of interest in view of previous findings that it is involved in stress response and that antibiotic biosynthesis in the genus is associated with development and occurs under stress conditions.

Here, we characterize HspR (SAV_4487) in *S. avermitilis* as a dual repressor/activator of avermectin production, development, and heat shock and H_2O_2 stress responses and identify HspR target genes associated with these biological processes. HspR interacted with PhoP at the *dnaK1* regulatory region to corepress the *dnaK1-grpE1-dnaJ1-hspR* operon. PhoP had exclusive target HSGs (*htpG*, *hsp18_1*, and *hsp18_2*) different from those of HspR (*clpB1p*, *clpB2p*, and *lonAp*). We propose a novel strategy for enhancing antibiotic production through overexpression of the *hspR* gene.

RESULTS

HspR represses *S. avermitilis* development but activates avermectin production. The gene *hspR* (*sav_4487*) in *S. avermitilis* contains 450 nucleotides (nt) and encodes a 16.8-kDa protein, HspR. The *S. avermitilis* chromosome has two copies of HSGs *dnaK*, *grpE*, and *dnaJ*. *hspR* is clustered with *dnaK1* (*sav_4484*), *grpE1* (*sav_4485*), and *dnaJ1* (*sav_4486*) to form the operon *dnaK1-grpE1-dnaJ1-hspR* (Fig. 1A). Protein alignment study showed that HspR is a highly conserved protein in *Streptomyces*; *S. avermitilis* HspR has 90.8%, 90.3%, 90.3%, 92%, and 90.8% amino acid identity with its homologs in *S. coelicolor*, *S. venezuelae*, *S. griseus*, *S. scabies*, and *S. lividans*, respectively, reflecting the biological importance of this protein in the genus.

To elucidate the functions of HspR in *S. avermitilis*, we constructed *hspR* deletion mutant Δ*hspR* (see Fig. S1 in the supplemental material), complemented strain C*hspR*, and overexpression strain O*hspR*. *hspR* transcription was undetectable in the Δ*hspR* strain as shown by reverse transcription and real-time quantitative PCR (RT-qPCR) analysis, and its levels were ~1.8-fold higher on day 2 (exponential phase) and ~3.1-fold higher on day 6 (stationary phase) in O*hspR* than in the wild-type (WT) strain (see Fig. S2), confirming the successful deletion or overexpression of *hspR* in the above-described strains.

The effect of HspR on morphological development was investigated by growing WT, Δ*hspR*, O*hspR*, and C*hspR* strains on solid sporulation yeast extract-malt-starch (YMS) plates. O*hspR* and C*hspR* strains were phenotypically similar to the WT, whereas the Δ*hspR* strain showed earlier and enhanced formation of spores (Fig. 1B). Spore numbers on days 2 and 4 were higher for the Δ*hspR* strain than for WT, as shown by scanning electron microscopy (SEM) (Fig. 1C). These findings indicate that HspR functions as a repressor during *S. avermitilis* development.

The effect of HspR on avermectin biosynthesis was investigated by high-performance liquid chromatography (HPLC) analysis of 10-day insoluble FM-I fermentation broth. In comparison to the WT value, the avermectin yield of the Δ*hspR* strain was ~43% lower, that of the O*hspR* strain was ~154% higher, and those of the C*hspR* and control strains (WT/pKC1139, WT/pSET152) were not significantly different (Fig. 1D and see Fig. S3). Time course measurements of growth in soluble FM-II showed that biomass (dry cell weight) values of the Δ*hspR* and O*hspR* strains were similar to that of the WT (Fig. 1E), ruling out the possibility that altered avermectin yields in the Δ*hspR* strain and the O*hspR* strain were due to changes in growth. These findings demonstrate that HspR functions as an activator in avermectin production.

In view of the finding that *hspR* overexpression increased avermectin yield in the WT, we transformed *hspR* overexpression vector pKC-*erm-hspR* into industrial strain A229 to construct O*hspR*/A229. Yield of avermectin B1a, the most effective component,

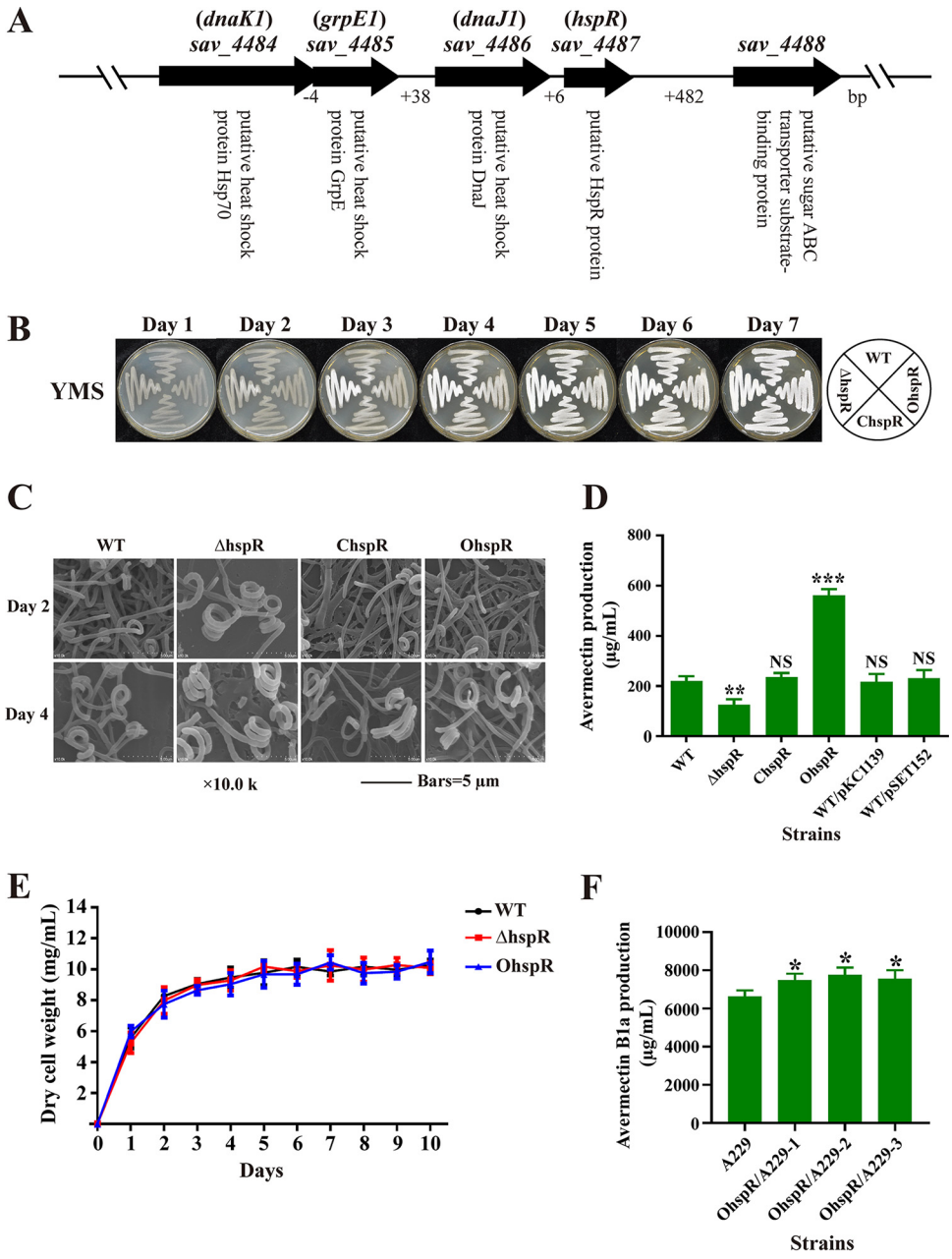

FIG 1 Effects of HspR on morphological development, avermectin production, and cell growth in *S. avermitilis*. (A) Genetic organization of the *dnaK1-grpE1-dnaJ1-hspR* operon. (B) Phenotypes of WT strain, the *hspR* deletion mutant (Δ*hspR*), complemented strain (*ChspR*), and overexpression strain (O*hspR*) grown on YMS agar at 28°C. (C) SEM images of WT, Δ*hspR*, *ChspR*, and O*hspR* strains grown on YMS agar for 2 or 4 days. (D) Avermectin yield in WT, Δ*hspR*, *ChspR*, O*hspR*, and control strains (WT/pKC1139 and WT/pSET152) after 10-day culture in FM-I. (E) Growth curves of WT, Δ*hspR*, and O*hspR* strains cultured in FM-II. (F) Avermectin yield in industrial strain A229 and its derivatives O*hspR*/A229-1, -2, and -3 (*hspR* overexpression strains) after 10-day culture in FM-I. Error bars (panels D, E, and F) indicate standard deviations (SDs) from three replicates. NS, not significant; *, $P < 0.05$; **, $P < 0.01$; ***, $P < 0.001$ for comparison with WT (D) or A229 (F) (Student's *t* test).

was ~14% to 17% higher for O*hspR*/A229 than in A229 (Fig. 1F). This finding indicates that avermectin yield could be substantially enhanced in high-producing industrial strains by *hspR* overexpression.

HspR directly activates *ave* structural genes. The transcription profile of *hspR* in FM-I culture of the WT was monitored by RT-qPCR to further clarify the regulatory role of HspR in avermectin production. The *hspR* transcription level increased to maximum on day 5, followed by a gradual decrease, and the level on day 7 was similar to that on

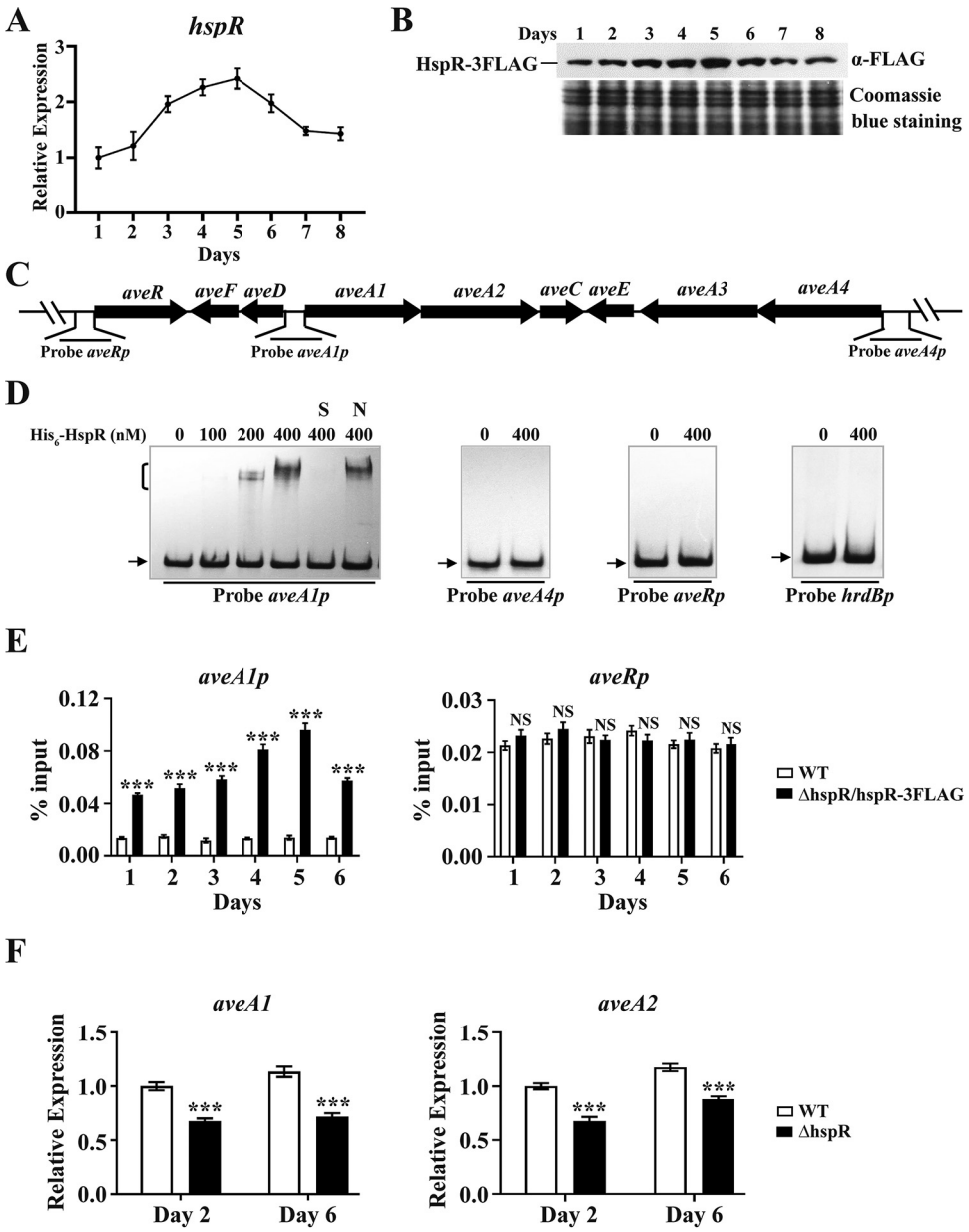

FIG 2 Direct activation of *aveA1-aveA2* by HspR. (A) RT-qPCR analysis of *hspR* transcriptional pattern in the WT grown in FM-I. The *hspR* transcription level on day 1 was set to 1. (B) Western blotting analysis of the HspR protein level during the fermentation process. The HspR expression level in strain Δ*hspR*/*hspR*-3FLAG grown in FM-I was determined using anti-FLAG MAb. (C) Schematic diagram of promoter probes used in EMSAs. (D) *In vitro* EMSAs of interactions of His_6-HspR with indicated probes (*hrdBp* as negative-control probe). A 0.15 nM concentration of labeled probe and various amounts of His_6-HspR were used for each binding reaction. In competition experiments, ~300-fold unlabeled nonspecific probe *hrdBp* (lane N) or specific probe *aveA1p* (lane S) was used. Arrows indicate free probes. Bracket indicates the HspR-DNA complex. (E) *In vivo* ChIP-qPCR assays of HspR binding to *aveA1p* and *aveRp* using Δ*hspR*/*hspR*-3FLAG and WT (negative control) strains grown in FM-II for the indicated times. The *y* axis indicates the relative binding level of HspR-FLAG on each site, determined by recovery of target sequence with anti-FLAG MAb. (F) RT-qPCR analysis of *aveA1* and *aveA2* in WT and Δ*hspR* strains grown in FM-I. WT value on day 2 for each gene was set to 1. Error bars (panels A, E, and F) indicate SDs from three replicates. NS, not significant; ***, $P < 0.001$ (*t* test).

day 8 (Fig. 2A). The HspR protein expression level was examined concurrently by Western blotting. Avermectin production in strain Δ*hspR*/*hspR*-3FLAG (fusion protein HspR-3FLAG expressed in the Δ*hspR* strain) was similar to that in the WT (see Fig. S4), indicating that HspR-3FLAG complemented HspR function and that the HspR expression profile could be examined using anti-FLAG antibody against HspR-3FLAG in the

Δ*hspR*/*hspR*-3FLAG strain. Consistent with the transcription profile, the HspR protein level was maximal on day 5 and then declined gradually (Fig. 2B). These findings suggest that HspR plays its regulatory role particularly during the middle fermentation stage or that there is something about this stage in growth that is particularly relevant to one of the stresses modulated by this protein.

To determine whether HspR regulates avermectin production through CSR gene *aveR* (29, 30) or structural genes, we performed a series of *in vitro* electrophoretic mobility shift assays (EMSAs) using soluble His_6-HspR expressed in and purified from *E. coli*. The four genes in the *ave* gene cluster (*aveA1*, *aveA2*, *aveA3*, and *aveA4*) encode polyketide synthases (PKSs) responsible for the synthesis of the avermectin polyketide backbone. *aveA1* is cotranscribed with *aveA2*, and *aveA4* is cotranscribed with *aveA3* (31). We therefore designed promoter probes *aveRp*, *aveA1p* (for *aveA1-aveA2*), and *aveA4p* (for *aveA4-aveA3*) for EMSAs (Fig. 2C) and used nonspecific probe *hrdBp* as the control. His_6-HspR clearly retarded *aveA1p* but did not bind to *aveA4p*, *aveRp*, or *hrdBp* (Fig. 2D). Binding specificity was confirmed by adding ~300-fold unlabeled specific probe *aveA1p* (lane S), which abolished the retarded band, or unlabeled nonspecific probe *hrdBp* (lane N), which had no effect on the delayed signal. Because of the cotranscription of *aveA1* and *aveA2*, *aveA2* is also targeted by HspR. These findings indicate that HspR directly regulates *ave* structural genes (*aveA1* and *aveA2*) but not CSR gene *aveR*.

In vivo binding of HspR to *aveA1p* was confirmed by chromatin immunoprecipitation-quantitative PCR (ChIP-qPCR) assays. Samples were taken from WT and Δ*hspR*/*hspR*-3FLAG strains grown in FM-II for various durations. HspR bound to *aveA1p* at various time points. Binding was strongest on day 5 (consistent with HspR expression profile), whereas HspR was not enriched on *aveRp* (Fig. 2E), indicating dynamic binding of HspR to the target promoter *aveA1p in vivo*.

The effect of HspR on expression of targeted *aveA1* and *aveA2* genes was assessed by RT-qPCR, using RNAs isolated from 2-day and 6-day FM-I cultures of WT and Δ*hspR* srains. *aveA1* and *aveA2* transcription levels were lower in the Δ*hspR* strain than in the WT on both days (Fig. 2F), consistent with avermectin yields for the strains, indicating that HspR activates transcription of these two genes.

Determination of precise HspR-binding site on the *aveA1* promoter region. To identify the precise HspR-binding site on *aveA1p* and clarify the mechanism whereby HspR regulates the *aveA1* gene, we performed DNase I footprinting assays. HspR protected a 31-nt region containing a 19-nt sequence (TTGAACGTCTTCAACTCTT) (Fig. 3A) similar to the conserved HspR-binding site HAIR in *S. coelicolor* (14), suggesting that the DNA-binding property of HspR is conserved.

The importance of the 19-nt HAIR-like sequence in HspR binding was evaluated by performing EMSAs using 50-nt probes that contained either the intact sequence (termed probe *aveA1p*-1) or the mutated sequence (termed probe *aveA1p*-1m; lacking inverted repeats) (Fig. 3B). His_6-HspR bound to WT probe *aveA1p*-1 but not to mutated probe *aveA1p*-1m (Fig. 3B), indicating that the 6-nt inverted repeats within the HAIR-like sequence are essential for HspR binding.

The transcriptional start site (TSS) of the *aveA1* gene was determined by our group previously (32), and −35 and −10 promoter sequences were predicted on this basis (Fig. 3C). The 19-nt HspR-binding site on *aveA1p* is very close to the −10 region (3 nt downstream) and overlaps the *aveA1* TSS (Fig. 3C). The HspR-binding site on *aveA1p* is unusual in regard to transcriptional activation; however, it is analogous to the binding sites of *Streptomyces* antibiotic regulatory protein (SARP)-family regulators AfsR (33) and OtcR (34), which are close to the −10 regions. These regulators presumably activate target transcription by recruiting RNA polymerase to the promoters. The mechanism of such activation of *aveA1* by HspR remains to be elucidated.

Identification of *S. avermitilis* HspR target HSGs. To examine response of HspR to heat shock stress in *S. avermitilis*, we measured the sensitivity of WT and Δ*hspR* strains to heat treatment. Growth of the Δ*hspR* strain was more resistant to heat shock stress

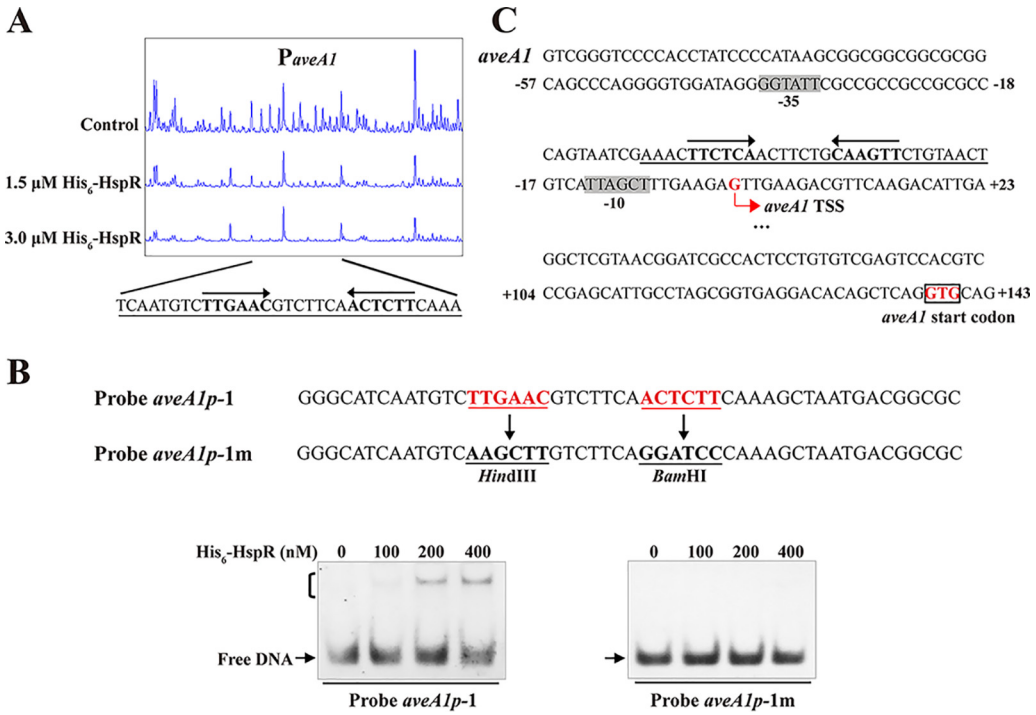

FIG 3 HspR-binding site on *aveA1* promoter region. (A) DNase I footprinting assay of HspR on *aveA1p*. Protection patterns were acquired with increasing His_6-HspR concentrations (reaction without His_6-HspR used as a control). (B) EMSAs using 50-nt WT probe *aveA1p*-1 and its mutated probe *aveA1p*-1m. Imperfect inverted repeats in probe *aveA1p*-1 were replaced with HindIII and BamHI sites to produce mutated probe *aveA1p*-1m. Each lane contained 0.15 nM labeled probe. (C) Nucleotide sequences of *aveA1* promoter region and HspR-binding site. Numbers indicate the distance (nucleotides) from *aveA1* TSS. Box, *aveA1* translational start codon (TSC); bent arrow, *aveA1* TSS; shading, probable −10 and −35 regions; solid line, HspR-binding site; straight arrows, inverted repeats.

than that of the WT (Fig. 4A), indicating that HspR represses the HSR, consistent with reported functions of its homologs in *S. coelicolor* and *S. albus* (13–16).

To identify HspR target HSGs, we performed EMSAs using His_6-HspR and promoter probes of potential HSGs based on the *S. avermitilis* genome database (http://avermitilis.ls.kitasato-u.ac.jp): *dnaK1p* (for the *dnaK1-grpE1-dnaJ1-hspR* operon), *dnaK2p* (for the *dnaK2-grpE2-dnaJ2* operon), *clpB1p*, *clpB2p*, *lonAp*, and *groES1p* (for the *groES1-groEL1* operon), *groEL2p*, *htpGp*, *hsp18_1p*, and *hsp18_2p* (Fig. 4B). His_6-HspR bound specifically to *dnaK1p*, *clpB1p*, *clpB2p*, and *lonAp* but not to other probes (Fig. 4C). *hspR* belongs to the *dnaK1-grpE1-dnaJ1-hspR* operon; therefore, HspR is autoregulated. Direct binding of HspR to *dnaK1p*, *clpB1p*, *clpB2p*, and *lonAp in vivo* was confirmed by ChIP-qPCR assays (Fig. 4D). Transcription levels of *dnaK1*, *hspR*, *clpB1*, *clpB2*, and *lonA* were shown by RT-qPCR analysis to be strongly upregulated in the Δ*hspR* strain on days 2 and 6 (Fig. 4E), indicating that HspR functions as a repressor of these target HSGs, consistent with the Δ*hspR* phenotype in heat stress assays.

To determine whether *dnaK1*, *hspR*, *clpB1*, *clpB2*, and *lonA* were induced in an HspR-dependent manner under heat stress, WT and Δ*hspR* strains were cultured in FM-II for 2 days, followed by heat (50°C) treatment for various durations. For the WT, heat treatment resulted in maximal induction of *dnaK1* (~49-fold), *hspR* (~43-fold), *clpB1* (~84-fold), *clpB2* (~1.4-fold), and *lonA* (~52-fold) within 10 min (see Fig. S5), indicating that HSPs DnaK1, ClpB1, and LonA play key roles in the HSR. For the Δ*hspR* strain, transcription levels of these five genes were all higher than the levels for the WT and also reached maximal values within 10 min of heat treatment. These findings confirm the negative role of HspR in controlling these target HSGs and suggest that these genes are also controlled by other regulator(s).

DNase I footprinting assays revealed that HspR protects two sites (*dnaK1*-I, *dnaK1*-II) on *dnaK1p* and that both sites contain a 19-nt HAIR-like sequence (Fig. 5A). The role of HAIR-

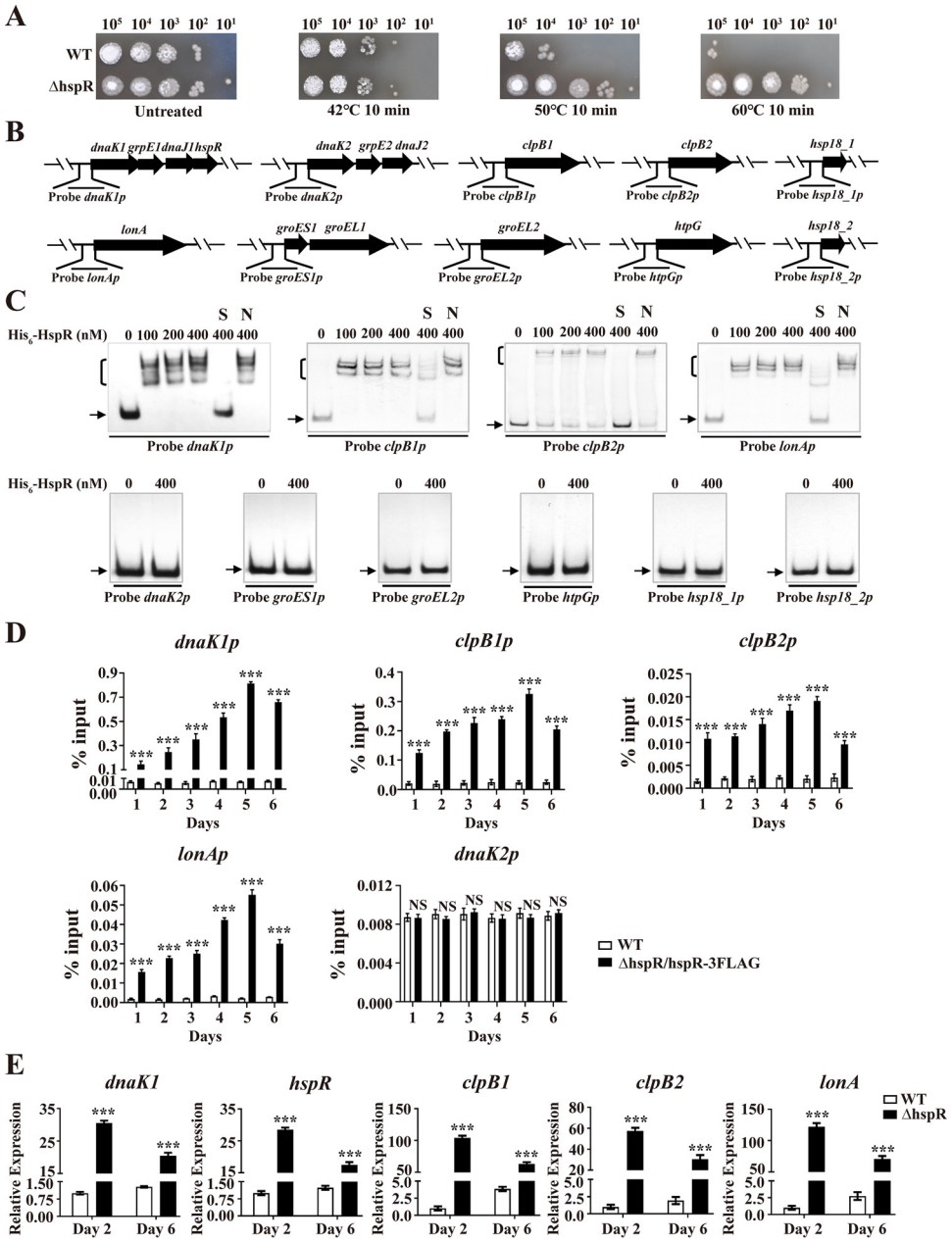

FIG 4 Identification of HspR target HSGs. (A) Sensitivity of WT and Δ*hspR* strains to heat stress. Spore suspensions were treated at 42°C, 50°C, or 60°C for 10 min, spotted on YMS agar, and photographed after 3-day growth at 28°C. (B) Promoter probes of HSGs used in EMSAs. (C) EMSAs of His_6-HspR with indicated probes. Notations as in Fig. 2D. (D) ChIP-qPCR assays of HspR binding to *dnaK1p*, *clpB1p*, *clpB2p*, *lonAp*, and *dnaK2p*. Notations as in Fig. 2E. (E) RT-qPCR analysis of five HspR target HSGs in WT and Δ*hspR* strains grown in FM-I. Error bars (panels D and E) indicate SDs from three replicates. ***, $P < 0.001$ (*t* test).

like sequences in HspR binding was investigated by site-directed mutagenesis of 50-bp WT probes *dnaK1p*-1 and *dnaK1p*-2 on the inverted repeats to generate mutated probes *dnaK1p*-1m and *dnaK1p*-2m, respectively (Fig. 5B). EMSAs revealed that His_6-HspR affinity for the mutated probes was abolished in comparison to that for the corresponding WT probes (Fig. 5B), reflecting an essential role of HAIR-like sequences in HspR binding. Site *dnaK1*-I extends from positions −63 to −39, and site *dnaK1*-II extends from positions −12 to +15 relative to the *dnaK1* TSS (35) (Fig. 5C). Site *dnaK1*-I is close to the putative −35 region, and site *dnaK1*-II overlaps the putative −10 region of the *dnaK1* promoter and *dnaK1* TSS, indicating that HspR represses *dnaK1* by blocking RNA polymerase access.

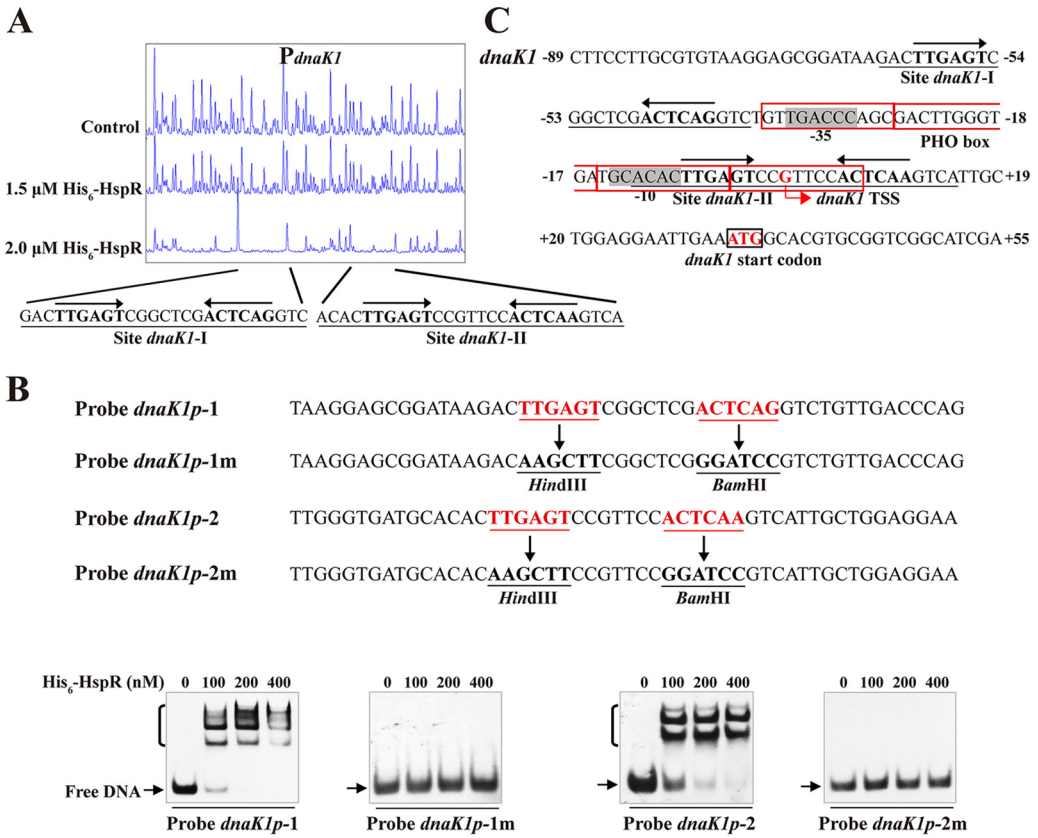

FIG 5 HspR-binding site on *dnaK1* promoter region. (A) DNase I footprinting assay of HspR on *dnaK1p*. (B) EMSAs using 50-nt WT probes *dnaK1p*-1 and *dnaK1p*-2 and their mutated probes *dnaK1p*-1m and *dnaK1p*-2m. Each lane contained 0.15 nM labeled probe. (C) Nucleotide sequences of *dnaK1* promoter region and HspR-binding sites. Numbers indicate distance (nucleotides) from *dnaK1* TSS. Black box, *dnaK1* TSC; bent arrow, *dnaK1* TSS; red boxes, PHO box. Other notations as in Fig. 3C.

The *clpB1*, *clpB2*, and *lonA* promoter regions also contain a 19-nt sequence similar to the HAIR motif, indicating that *S. avermitilis* HspR binds to these target DNAs at HAIR sites.

HspR responds to H_2O_2 stress. Possible regulation of other types of stress response by *S. avermitilis* HspR was evaluated on YMS plates. Relative to that of the WT, the Δ*hspR* strain showed greater sensitivity to H_2O_2 (which causes peroxidative stress) but similar sensitivity to *tert*-butyl hydroperoxide (TBHP; causes organic peroxidative stress), diamide (causes thiol-oxidative stress), and NaCl and KCl (cause osmotic stress) (Fig. 6A). *S. avermitilis* HspR evidently plays a role in resistance to H_2O_2 stress.

Bacteria typically respond to H_2O_2 stress by producing peroxidases and catalases that degrade H_2O_2. In *S. avermitilis*, one *ahpCD* operon (for alkyl hydroperoxide reductase and alkylhydroperoxidase), three catalase genes (*katA1*, *katA2*, and *katA3*), and two TR genes (*oxyR* and *catR*) are involved in H_2O_2 stress response (36). Possible interactions of His_6-HspR with promoter probes of these H_2O_2 stress-related genes (Fig. 6B) were investigated by EMSAs. His_6-HspR bound specifically to probe *katA3p* and bidirectional promoter probes *catR_katA1* and *oxyR_ahpCD* but not to *katA2p* (Fig. 6C). HspR-binding promoter regions *katA3p*, *catR_katA1*, and *oxyR_ahpCD* all contained HAIR-like sequences, as expected. Direct binding of HspR to *katA3p*, *catR_katA1*, and *oxyR_ahpCD* was confirmed *in vivo* by ChIP-qPCR assays (Fig. 6D). Consistent with the H_2O_2 stress phenotype for the Δ*hspR* strain, transcription levels of *katA1*, *catR*, *katA3*, *oxyR*, *ahpC*, and *ahpD* were all reduced in the Δ*hspR* strain relative to that in the WT grown in FM-I (Fig. 6E), indicating that HspR acts as an activator of these genes.

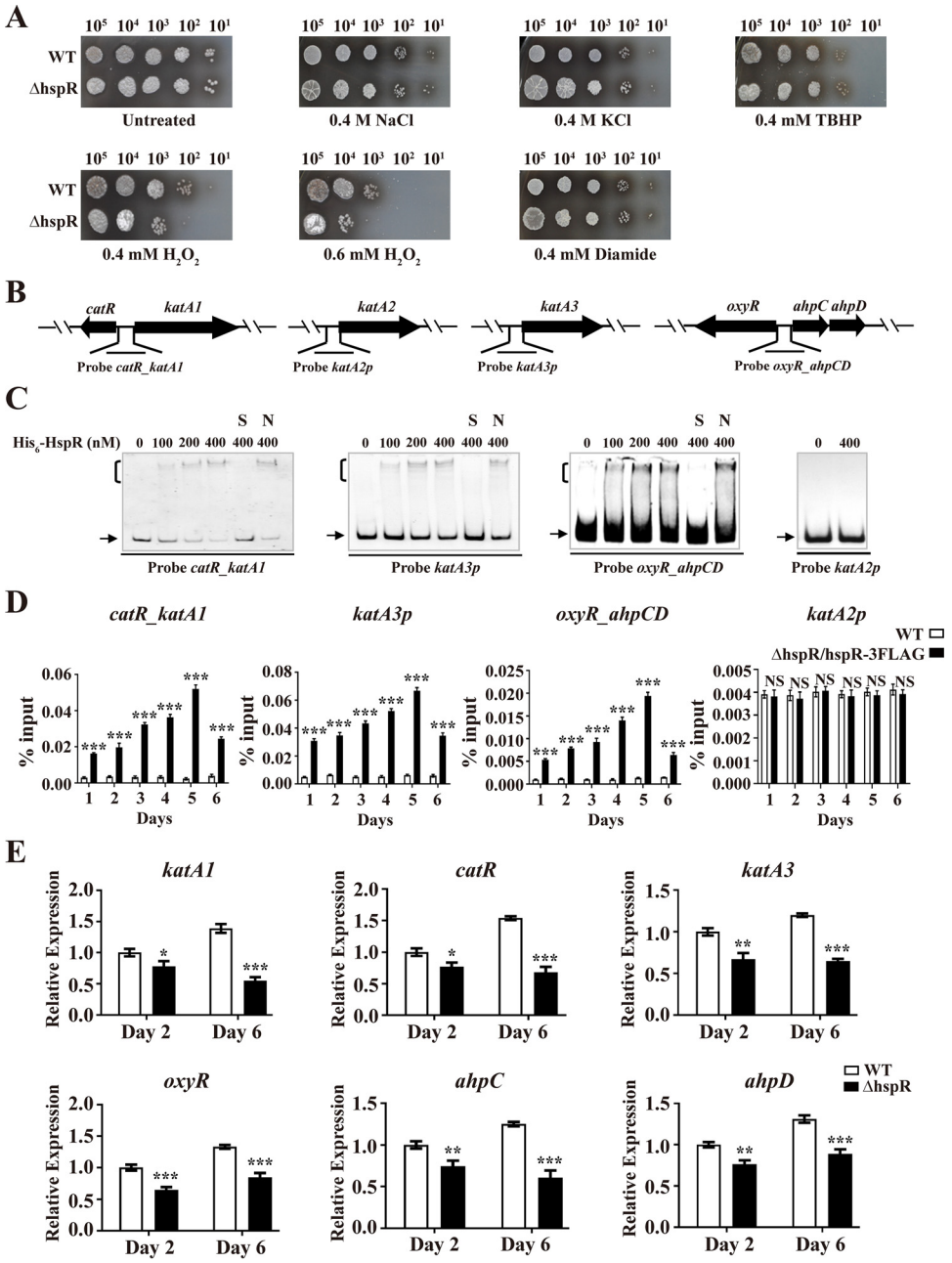

FIG 6 Identification of HspR target genes involved in H_2O_2 stress response. (A) Sensitivity of WT and Δ*hspR* strains to various stress conditions. Spore suspensions were diluted serially and spotted on YMS agar containing NaCl, KCl, TBHP, H_2O_2, or diamide at the indicated concentrations. (B) Promoter probes of H_2O_2 stress-related genes used in EMSAs. (C) EMSAs of His_6-HspR with indicated probes. Notations as in Fig. 2D. (D) ChIP-qPCR assays of HspR binding to *katA2p*, *katA3p*, *catR_katA1*, and *oxyR_ahpCD*. Notations as in Fig. 2E. (E) RT-qPCR analysis of six HspR target H_2O_2 stress-related genes in WT and Δ*hspR* strains grown in FM-I. Error bars (panels D and E) indicate SDs from three replicates. *, $P < 0.05$; **, $P < 0.01$; ***, $P < 0.001$ (*t* test).

For analysis of H_2O_2 stress responses, WT and Δ*hspR* strains were treated with 0.6 mM H_2O_2 for various durations. In the WT, H_2O_2 treatment caused notable induction of *katA1* (~47-fold) and *catR* (~8.7-fold) within 10 min and slight induction of *katA3* (~2.7-fold), *ahpC* (~1.39-fold), and *ahpD* (~1.36-fold) within 30 min and of *oxyR* (~2.2-fold) within 40 min, whereas H_2O_2 treatment of the Δ*hspR* strain had a much lower inducing effect on *katA1* (~5-fold), *catR* (~4.6-fold), and *oxyR* (~1.7-fold) and no effect on *katA3*, *ahpC*, or *ahpD* expression (see Fig. S6). These findings indicate that HspR

promotes H_2O_2 stress resistance in *S. avermitilis* by activating transcription of target genes (*katA1*, *catR*, *katA3*, *oxyR*, *ahpC*, and *ahpD*).

The effect of H_2O_2 on avermectin production was also investigated by HPLC analysis of 10-day cultures of the WT in FM-I containing various concentrations of H_2O_2, and the results showed that H_2O_2 addition did not promote avermectin production (see Fig. S7).

HspR interacts with PhoP at the *dnaK1* promoter region. Cross talk between different regulatory systems commonly occurs in bacteria for the coordination of cell growth and metabolism. In *M. tuberculosis*, HspR interacts with PhoP to coregulate expression of *acr2*, which encodes an essential pathogenic determinant (20). We examined the possibility that HspR also interacts with PhoP in *Streptomyces*. The *Streptomyces* PhoP-binding sequence (termed PHO box) consists of 11-nt consecutive direct repeat units (DRus; $G^{G/T}TCAYYYR^{G/C}G$) (37). We found that *dnaK1p* contains a PHO box sequence formed by four DRus and that the PHO box overlaps site *dnaK1*-II (Fig. 5C), suggesting that HspR-PhoP interaction may occur at *dnaK1p*. To test this possibility, we coexpressed His_6-HspR with glutathione transferase (GST) or GST-PhoP in *E. coli* and performed GST pulldown assays. His_6-HspR was pulled down by GST-PhoP but not by GST tag (negative control) (Fig. 7A), indicating that HspR interacts with PhoP. Specific binding of purified GST-PhoP (38) to *dnaK1p* was confirmed by EMSAs (Fig. 7B).

The PhoP-binding site on *dnaK1p* (PHO box) overlaps the HspR-binding site *dnaK1*-II; these two regulators may therefore affect each other's binding to *dnaK1p*. We examined this possibility by applying His_6-HspR and GST-PhoP, both separately and together, with probe *dnaK1p* in EMSAs. When applied separately, both proteins retarded *dnaK1p* migration (Fig. 7C). In the presence of 2 μM GST-PhoP, increasing amounts of His_6-HspR resulted in a reduction of the PhoP-*dnaK1p* complex, an increase of the HspR-*dnaK1p* complex, and formation of a new retarded band located between those for PhoP-*dnaK1p* and HspR-*dnaK1p* (Fig. 7C, left), which was presumably formed by interaction of the HspR-PhoP complex with *dnaK1p*. In the presence of 0.05 μM His_6-HspR, increasing amounts of GST-PhoP resulted in reduction of the HspR-*dnaK1p* complex, appearance of PhoP-*dnaK1p*, and appearance of a new band, presumably HspR-PhoP-*dnaK1p* (Fig. 7C, right). These findings suggest that HspR and PhoP cooperate as a complex for DNA binding besides competing for binding to *dnaK1p*.

We used ChIP-qPCR assays to examine binding of HspR-3FLAG to *dnaK1p* in WT, Δ*hspR*/*hspR*-3FLAG, WT/*hspR*-3FLAG, and Δ*phoP*/*hspR*-3FLAG strains. HspR-3FLAG on *dnaK1p* was enriched (relative to that for negative-control WT) in Δ*hspR*/*hspR*-3FLAG, WT/*hspR*-3FLAG, and Δ*phoP*/*hspR*-3FLAG strains grown in FM-II for various durations (Fig. 7D), indicating that DNA-binding activity of HspR does not depend on PhoP. Enrichment levels of HspR-3FLAG on *dnaK1p* were highest in the Δ*hspR*/*hspR*-3FLAG strain and higher in the Δ*phoP*/*hspR*-3FLAG strain than in the WT/*hspR*-3FLAG strain at various time points (Fig. 7D), indicating competitive binding of HspR and PhoP to *dnaK1p*. HspR evidently plays a dominant role relative to PhoP in the regulation of *dnaK1p*.

PhoP represses target HSGs. The observed binding of PhoP to *dnaK1p* suggests that PhoP may also be involved in the HSR. We evaluated this possibility by comparing the growth of WT and Δ*phoP* strains (38) on YMS plates following heat treatment. Resistance to heat shock stress was greater for the Δ*phoP* strain than for the WT (Fig. 8A), indicating that PhoP (like HspR) has a negative effect on HSR. In contrast to HspR, PhoP had no effect on the H_2O_2 stress response (Fig. 8A).

PhoP bound to probe *dnaK1p* (Fig. 7B). EMSAs with GST-PhoP and other promoter probes of HSGs (Fig. 4B) revealed specific binding of PhoP to *htpGp*, *hsp18_1p*, and *hsp18_2p* but not to other tested probes (Fig. 8B). HspR and PhoP thus have exclusive target HSGs in addition to their common target HSGs (genes in the *dnaK1-grpE1-dnaJ1-hspR* operon); i.e., *clpB1*, *clpB2*, and *lonA* are targets of HspR but not of PhoP, whereas *htpG*, *hsp18_1*, and *hsp18_2* are targets of PhoP but not of HspR.

Consistent with the Δ*phoP* phenotype observed in heat stress tests, transcription levels of PhoP target HSGs *dnaK1*, *hspR*, *htpG*, *hsp18_1*, and *hsp18_2* were much higher

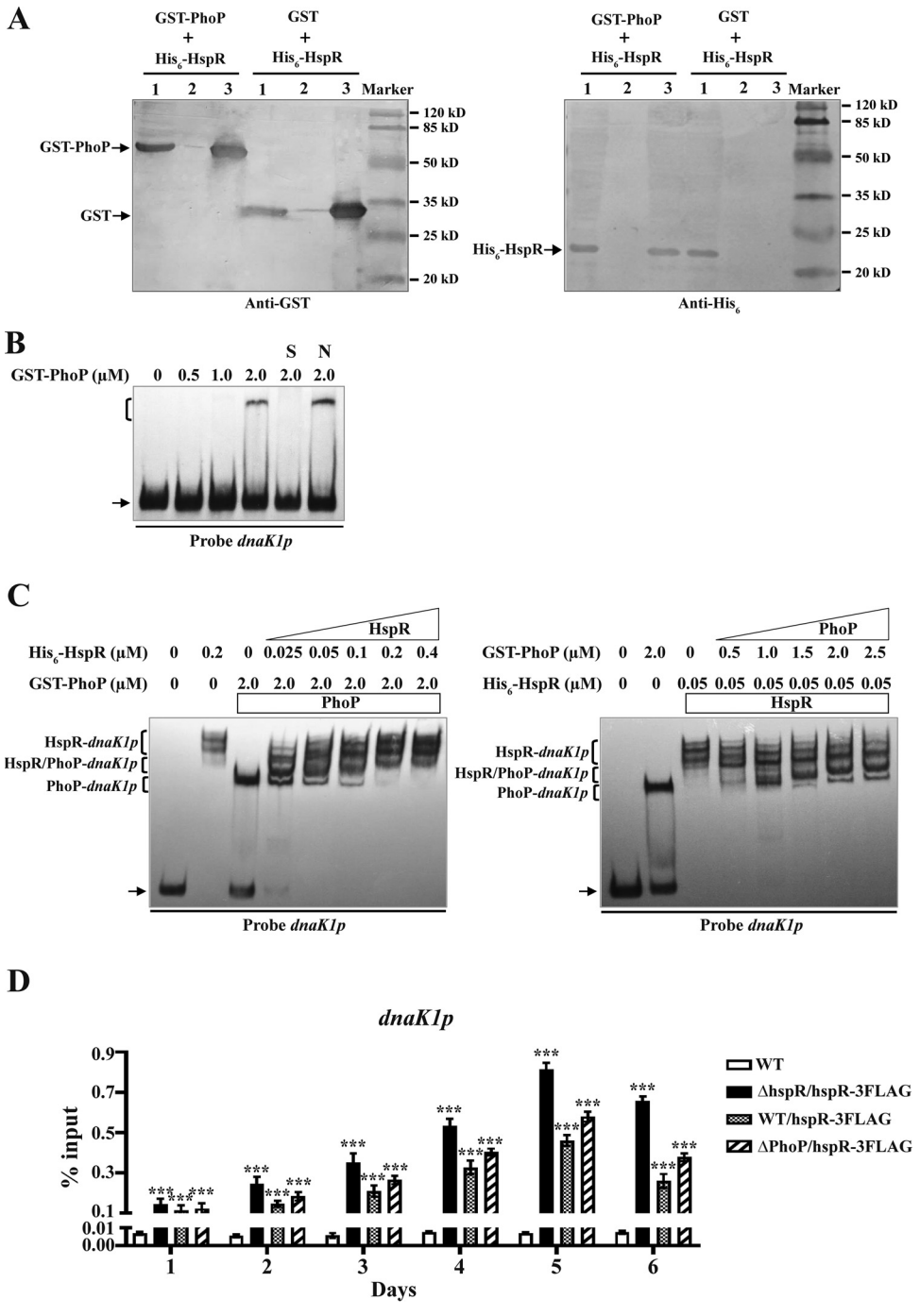

FIG 7 Interaction of HspR with PhoP at *dnaK1p*. (A) GST pulldown assays of HspR and PhoP from *E. coli* whole-cell lysate containing both His_6- and GST-tagged proteins. Lane 1, flowthrough of cell lysate after incubation with glutathione-Sepharose beads; lane 2, washing buffer following fourth wash of beads; lanes 3, GST pulldown. (B) EMSAs of GST-PhoP with probe *dnaK1p*. A 0.15 nM concentration of labeled probe and various amounts of GST-PhoP were used for each binding reaction. For nonspecific (lane N) or specific (lane S) competition assays, ~500-fold unlabeled competitor DNA was used. (C) Competitive EMSAs of probe *dnaK1p* with His_6-HspR and GST-PhoP. A 0.15 nM concentration of labeled probe *dnaK1p* was incubated with indicated concentrations of His_6-HspR and GST-PhoP. (D) ChIP-qPCR assays of HspR-3FLAG binding to *dnaK1p* in WT (negative control), Δ*hspR*/*hspR*-3FLAG, WT/*hspR*-3FLAG, and Δ*phoP*/*hspR*-3FLAG strains grown in FM-II for the indicated times. Error bars indicate SDs from three replicates. ***, $P < 0.001$ (*t* test).

in the Δ*phoP* strain than in the WT grown in FM-I (Fig. 8C), indicating negative regulation of these targets by PhoP. Transcription levels of these five genes in WT and Δ*phoP* strains were recorded under heat shock stress. In the WT, levels increased to maximum for *dnaK1* (~49-fold) and *hspR* (~43-fold) within 10 min, for *hsp18_1* (~22-fold) and

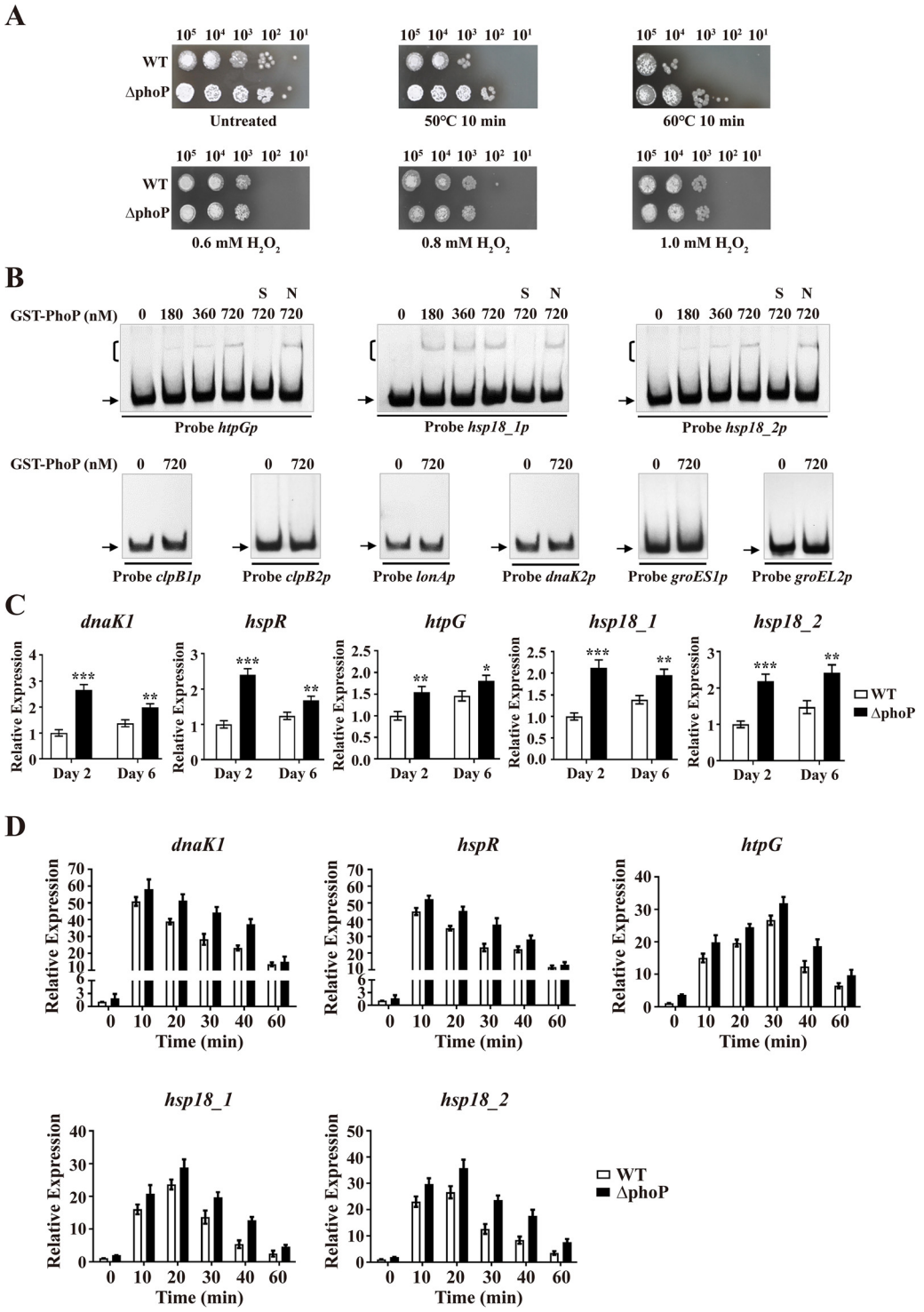

FIG 8 Identification of PhoP target HSGs. (A) Sensitivity of WT and Δ*phoP* strains to heat and H_2O_2 stresses. (B) EMSAs of GST-PhoP with promoter probes of HSGs. Notations as in Fig. 7B. (C) RT-qPCR analysis of five PhoP target HSGs in WT and Δ*phoP* strains grown in FM-I. *, $P < 0.05$; **, $P < 0.01$; ***, $P < 0.001$ (*t* test). (D) Induction of five HSGs by heat treatment (50°C) in WT and Δ*phoP* strains grown in FM-II. For each gene, the transcription level in the WT before temperature rise (0 min) was set to 1. Error bars (panels C and D) indicate SDs from three replicates.

hsp18_2 (~25-fold) within 20 min, and for *htpG* (~25-fold) within 30 min (Fig. 8D), indicating important roles of DnaK1, Hsp18_1, Hsp18_2, and HtpG in HSR. In the Δ*hspR* strain, all five genes showed increased transcription levels (Fig. 8D), confirming repression of these genes by PhoP.

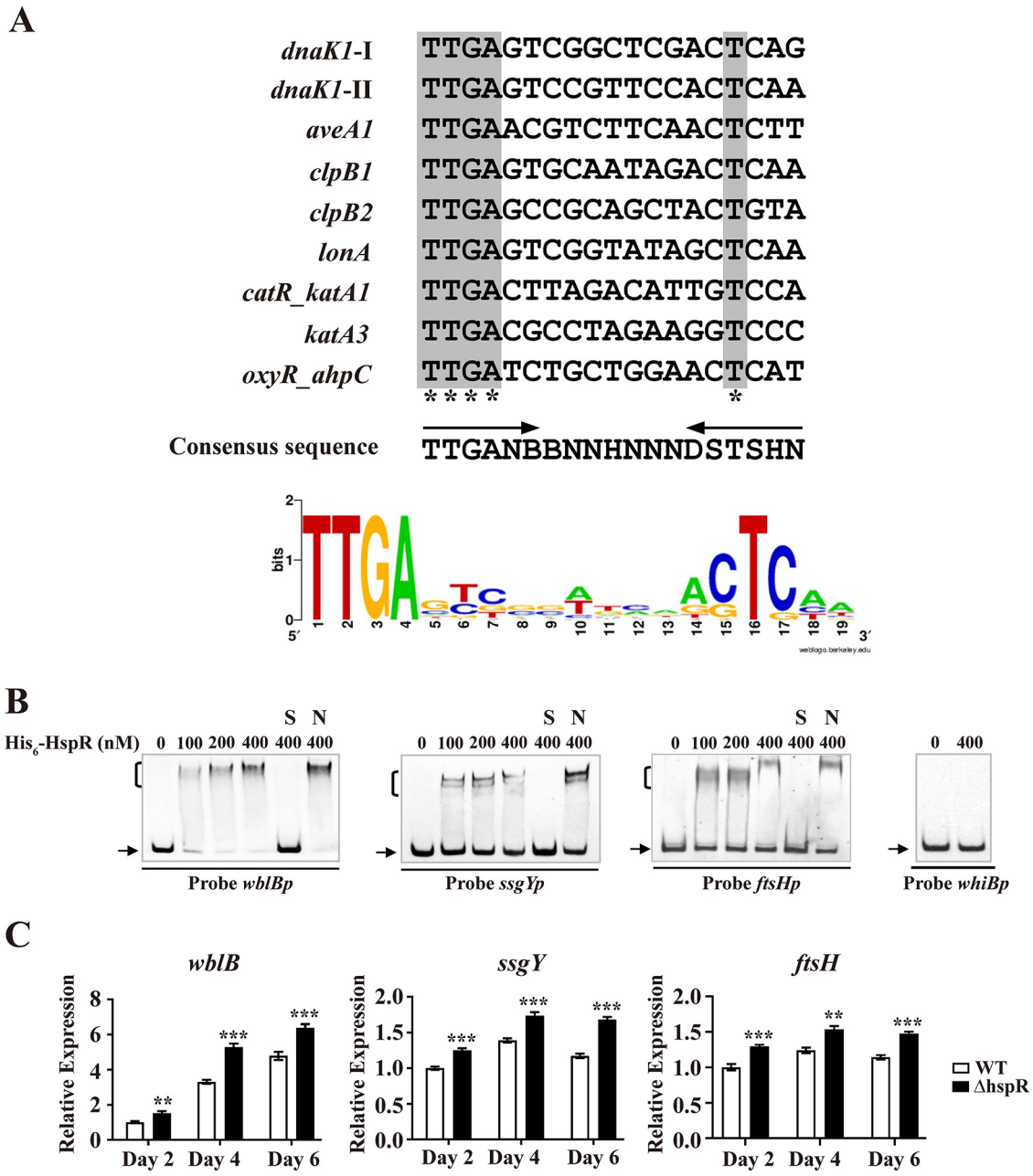

FIG 9 Identification of HspR target genes associated with development. (A) Analysis of consensus HspR-binding sequence by WebLogo. Arrows, conserved 6-nt inverted repeats; asterisks, consensus bases. (B) EMSAs of His_6-HspR with promoter probes of four developmental genes. Notations as in Fig. 2D. (C) RT-qPCR analysis of *wblB*, *ssgY*, and *ftsH* in WT and Δ*hspR* strains grown on YMS agar. Error bars show SDs from three replicates. **, $P < 0.01$; ***, $P < 0.001$ (*t* test).

Prediction of HspR regulon and identification of HspR targets involved in development. To further clarify the roles of HspR in *S. avermitilis*, we predicted its regulon. WebLogo (http://weblogo.berkeley.edu) analysis of the 19-nt HAIR sequences in the above-mentioned HspR-binding promoter regions (*aveA1p*, *dnaK1p*, *clpB1p*, *clpB2p*, *lonAp*, *catR-katA1*, *katA3p*, and *oxyR-ahpCD*) revealed a consensus sequence, 5′-TTGANBBNNHNNNDSTSHN-3′ (N is A/T/C/G, B is T/C/G, H is A/C/T, D is A/G/T, and S is C/G) (Fig. 9A). Scanning of the *S. avermitilis* genome with the 19-nt consensus HspR-binding sequence by PREDetector (39) identified 155 putative HspR target genes (cutoff; score ≥ 8) (see Table S1). Of these, 60 were unclassified or unknown, and the remaining 95 were assigned to 15 functional groups on the basis of the KEGG pathway database for *S. avermitilis*.

Our phenotypic observations revealed the negative role of HspR in *S. avermitilis* development. We therefore performed EMSAs on several predicted HspR target developmental genes listed in Table S1: *whiB* (*sav_5042*) for sporulation regulator WhiB (40), *wblB* (*sav_4997*) for putative WhiB-family TR (putative control of cell cycle), *ssgY* (*sav_4267*) for putative sporulation-specific cell division protein SsgY, and *ftsH* (*sav_4666*) for putative cell division protein FtsH. His_6-HspR bound to promoter probes *wblBp*, *ssgYp*, and *ftsHp* but not to probe *whiBp* (Fig. 9B). Transcription levels of *wblB*, *ssgY*, and *ftsH* were determined by RT-qPCR using RNAs prepared from WT and Δ*hspR* strains grown on YMS plates for 2 (aerial hypha growth stage), 4 (middle sporulation stage), or 6 (spore maturation stage) days. Levels of these three genes were higher in the Δ*hspR* strain than in the WT at three time points (Fig. 9C), consistent with the earlier differentiation phenotype of the Δ*hspR* strain. These findings indicate that HspR negatively regulates development by directly repressing *wblB*, *ssgY*, and *ftsH*.

DISCUSSION

HspR has been reported to function as an HSR repressor in *S. coelicolor*, *S. albus*, and *S. lividans* (13–17); however, its roles in antibiotic production, development, and other stress responses of *Streptomyces* had not been studied until now. Results of the present study of molecular mechanisms underlying HspR function in avermectin production, development, and heat shock and H_2O_2 stress responses in *S. avermitilis* demonstrate that HspR acts as a dual repressor/activator in these important physiological processes through control of corresponding target genes. HspR was shown to interact with another important regulator, PhoP, to coregulate the HSR. These findings bring to light previously unrecognized roles and regulatory mechanisms of HspR in this genus and provide a basis for the construction of antibiotic-overproducing strains in *Streptomyces* species.

S. avermitilis HspR directly activated avermectin production by interacting with the promoter region of structural genes *aveA1* and *aveA2* and strongly promoted avermectin production in both WT and industrial strains. HspR homologs are widely distributed among *Streptomyces*. The HspR-mediated activation of antibiotic production may occur in other *Streptomyces* species, and this possibility requires further investigations.

HspR was shown to play a negative regulatory role in *S. avermitilis* development, and three developmental genes (*wblB*, *ssgY*, and *ftsH*) were identified as HspR targets. *wblB* encodes a putative WhiB-family TR homologous to *S. coelicolor* WhiD, which is required for late-stage sporulation (41). *ssgY* encodes a putative cell division protein homologous to *S. coelicolor* SsgA, which is required for synthesis of sporulation septa (42). *ftsH* encodes a putative cell division protein homologous to *E. coli* FtsH. Enhanced expression of these three HspR target genes in the Δ*hspR* strain may account for the phenotype of this mutant. However, we cannot rule out possible contributions to the Δ*hspR* phenotype by other HspR target developmental genes; further studies are needed to resolve this point.

In regard to control of the HSR, *S. avermitilis* HspR acts as a direct repressor of several HSGs (the *dnaK1-grpE1-dnaJ1-hspR* operon, *clpB1p*, *clpB2p*, and *lonAp*), consistent with its reported role in HSRs in other *Streptomyces* species (13–17). The ability of HspR and chaperone DnaK to form a complex to corepress HspR target HSGs has been well established in *S. coelicolor* (14, 18). HspR and DnaK are both highly conserved in the genus, and it is therefore likely that HspR-DnaK interaction occurs in other species. The mechanism of such interaction was not investigated in the present study. Our findings reveal an additional layer of complex regulation of HSR, i.e., HspR cross talks with PhoP at *dnaK1p* to corepress the *dnaK1-grpE1-dnaJ1-hspR* operon. GST pulldown and competitive EMSAs revealed the existence of the HspR-PhoP complex and the reduction or disappearance of the HspR-PhoP-*dnaK1p* complex with increasing concentrations of one protein while concentration of the other protein remained constant, indicating that formation of the HspR-PhoP complex is a highly dynamic process. HspR and PhoP do not depend on each other for DNA binding, and they both have exclusive target

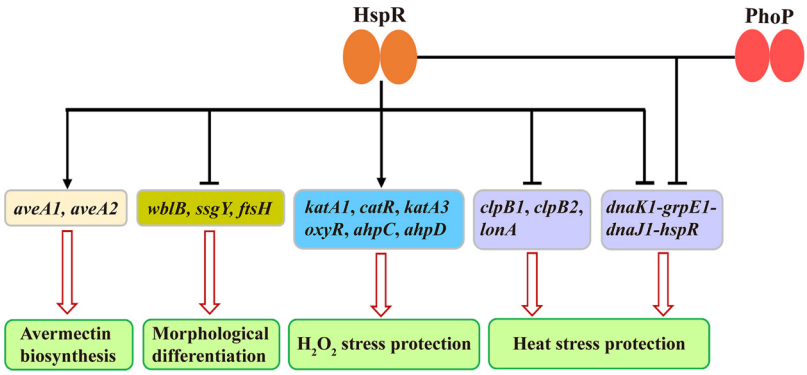

FIG 10 Proposed model of HspR-mediated regulatory network in *S. avermitilis*. Solid arrows, direct activation; bars, direct repression; hollow arrows, avermectin biosynthesis, development, or response to stress.

HSGs (*clpB1*, *clpB2*, and *lonA* for HspR; *htpG*, *hsp18_1*, and *hsp18_2* for PhoP). The HspR-PhoP complex may therefore play a regulatory role which neither protein by itself is capable; i.e., stabilization of DNA-protein structure to precisely regulate essential genes. Consistent with this possibility, the essential pathogenic determinant gene *acr2* in *M. tuberculosis* is regulated by the HspR-PhoP complex (20). Notwithstanding their cooperative activity, HspR and PhoP compete for binding to *dnaK1p*, i.e., an increasing concentration of one protein suppresses formation of the complex with *dnaK1p* by the other protein, reflecting the delicate interplay between these two regulators in the control of the *dnaK1-grpE1-dnaJ1-hspR* operon. Our findings reveal a novel role of PhoP in the HSR and further demonstrate the importance of PhoP in *Streptomyces*. Coregulation of the *dnaK1-grpE1-dnaJ1-hspR* operon by HspR and PhoP suggests that HSGs within this operon play a dominant role over other HSGs in response to heat shock stress.

HspR has a negative regulatory role in the HSR, but we also observed a positive role in the H_2O_2 stress response, i.e., it directly activates the transcription of related genes. HspR target genes (*katA1*, *catR*, *katA3*, *oxyR*, *ahpC*, and *ahpD*) are well conserved in *Streptomyces*; such an HspR-based mechanism involved in the control of the H_2O_2 stress response is therefore likely to be present in other species. HspR also functions as an activator (it activates transcription of *ave* structural genes and H_2O_2 stress-related genes), but the mechanism underlying this function remains to be elucidated.

Our findings, taken together, provide a basis for a proposed model of the HspR-mediated regulatory network involved in development, avermectin production, and heat shock and H_2O_2 stress responses in *S. avermitilis* (Fig. 10). These important physiological processes are coordinated by HspR through its positive or negative effect on target genes. HspR also interacts with PhoP to corepress the *dnaK1-grpE1-dnaJ1-hspR* operon. Predicted HspR targets are involved in other essential functions such as primary metabolism (see Table S1 in the supplemental material). It is clear that the roles of HspR in *Streptomyces* are much broader than previously recognized. Identification of additional targets and related molecular processes will require extensive further study.

MATERIALS AND METHODS

Strains, plasmids, primers, and growth conditions. Strains and plasmids used in this study are listed in Table 1, and primers are listed in Table 2. Culture conditions for *S. avermitilis* and *E. coli* were described previously (43). YMS (44) agar was used for observation of the *S. avermitilis* phenotype. Insoluble FM-I fermentation medium and soluble FM-II fermentation medium (45) were used for routine avermectin production and growth analysis, respectively. FM-II was also used to grow mycelia for ChIP-qPCR assays and for RNA isolation following stress treatment.

Construction of *S. avermitilis* mutant strains. To construct the *hspR* deletion mutant, a 594-bp 5′ flanking region (positions −527 to +67 relative to the *hspR* translational start codon [TSC]) and a 454-bp 3′ flanking region (positions +385 to +838) were generated by PCR from *S. avermitilis* WT genome with

TABLE 1 Strains and plasmids used in this study

Strain or plasmid	Description	Source or reference
Strains		
S. avermitilis		
ATCC 31267	Wild-type (WT) strain	Laboratory stock
A229	Industrial strain	Qilu Pharmaceutical
Δ*hspR*	*hspR* deletion mutant	This study
C*hspR*	*hspR* complemented strain	This study
O*hspR*	*hspR* overexpression strain	This study
Δ*phoP*	*phoP* deletion mutant	38
Δ*hspR*/*hspR*-3FLAG	*hspR* complemented strain with HspR-3FLAG	This study
Δ*phoP*/*hspR*-3FLAG	*phoP* deletion mutant with HspR-3FLAG	This study
WT/*hspR*-3FLAG	WT strain with HspR-3FLAG	This study
WT/pKC1139	WT strain carrying empty vector pKC1139	This study
WT/pSET152	WT strain carrying empty vector pSET152	This study
O*hspR*/A229	*hspR* overexpression strain based on A229	This study
E. coli		
JM109	General cloning host for plasmid manipulation	Laboratory stock
BL21(DE3)	Host for protein expression	Novagen
Plasmids		
pKC1139	Multiple-copy temperature-sensitive *E. coli-Streptomyces* shuttle vector	46
pSET152	Integrative *E. coli-Streptomyces* shuttle vector	46
pET-28a(+)	Vector for His_6-tagged protein expression in *E. coli*	Novagen
pGEX-4T-1	Vector for GST-tagged protein expression in *E. coli*	GE Healthcare
pCIMt005	Multiple-copy temperature-sensitive *E. coli-Streptomyces* shuttle vector	47
pJL117	pIJ2925 derivative carrying the *Streptomyces* strong constitutive promoter *ermE*p*	49
pKCΔ*hspR*	*hspR* deletion vector based on pKC1139	This study
pΔ*hspR*	*hspR* deletion vector based on pCIMt005	This study
pSET152-*hspR*	*hspR* complemented vector based on pSET152	This study
pKC-*erm*-*hspR*	*hspR* overexpression vector based on pKC1139	This study
pSET152-*hspR*-3FLAG	*hspR* complemented vector with 3×FLAG-tagged HspR on pSET152	This study
pIJ10500	Vector carrying 3×FLAG fragment	50
pET28-*hspR*	His_6-HspR expression vector based on pET-28a(+)	This study
pGEX-*phoP*	GST-PhoP expression vector based on pGEX-4T-1	38

primers WQ11/WQ12 and WQ13/WQ14. The two fragments were digested with BamHI/XbaI and XbaI/HindIII, respectively, and then ligated into BamHI/HindIII-digested pKC1139 (46) to generate pKCΔ*hspR*. Temperature-sensitive plasmid pCIMt005, containing the *idgS* gene that encodes indigoidine synthetase to make colonies blue, was used for *hspR* deletion by simple blue-white screening (47). A 1,048-bp DNA fragment containing 5′- and 3′-flanking regions of *hspR* was amplified from pKCΔ*hspR* with primers LXR101A and LXR101B and ligated into NcoI-digested pCIMt005 to generate *hspR* deletion vector pΔ*hspR*, which was transformed into WT protoplasts. The *hspR* deletion mutant was screened as described previously (48) and confirmed by colony PCR and DNA sequencing. Use of primers WQ15 and WQ16 (flanking the exchange regions) (see Fig. S1 in the supplemental material) resulted in the appearance of a 1,337-bp band, whereas a 1,655-bp band was observed in the WT. When primers WQ17 and WQ18 (located within the deletion region of *hspR*) were used, only the WT produced a 385-bp band. We thus generated the *hspR* deletion mutant (Δ*hspR* strain), in which a 275-bp fragment within *hspR* open reading frame (ORF) (positions +112 to +386 relative to the TSC) was deleted (see Fig. S1).

For complementation of Δ*hspR*, a 465-bp fragment containing the *hspR* ORF and a 446-bp fragment containing the *dnaK1* promoter were amplified with primers LXR134A/LXR134B and LXR133A/LXR133B, respectively. The two PCR fragment were digested with BamHI/HindIII and EcoRI/BamHI, respectively, and ligated simultaneously into pSET152 (46) to generate *hspR*-complemented vector pSET152-*hspR*, which was then introduced into the Δ*hspR* strain to generate complemented strain C*hspR*.

For overexpression of *hspR*, a 586-bp fragment carrying the *hspR* ORF was amplified with primers WQ25 and WQ26 and ligated simultaneously with a 188-bp *ermE*p* (*Streptomyces* strong constitutive promoter) fragment from pJL117 (49) into pKC1139 to generate *hspR*-overexpressing vector pKC-*erm*-*hspR*, which was introduced into *S. avermitilis* WT and industrial strain A229 to generate *hspR* overexpression strains O*hspR* and OhspR/A229, respectively.

To express 3×FLAG-tagged HspR in *S. avermitilis*, the *hspR* ORF and *dnaK1* promoter were amplified with primers LXR135A/LXR135B and LXR136A/LXR136B from WT genomic DNA, and the 3×FLAG fragment was amplified with primers LXR60A and LXR60B from plasmid pIJ10500 (50). The resulting 453-bp *hspR*, 446-bp *dnaK1* promoter, and 100-bp FLAG fragments were cloned into pSET152 to generate pSET152-*hspR*-3FLAG, which was then transformed into WT, Δ*hspR*, and Δ*phoP* strains to generate recombinant strains WT/*hspR*-3FLAG, Δ*hspR*/*hspR*-3FLAG, and Δ*phoP*/*hspR*-3FLAG strains, respectively, for expression of C-terminally 3×FLAG-tagged HspR.

TABLE 2 Primers used in this study

Primer	DNA sequence[a] (5′→3′)	Use
Gene disruption, complementation, and overexpression		
WQ11	CGGGATCCGATCGCCGAGAACCCCTG (BamHI)	Deletion of *hspR* gene
WQ12	GCTCTAGAGTACTGACGCAGGGTCTG (XbaI)	
WQ13	GCTCTAGAACCAGGAGGTCCAGCAGA (XbaI)	
WQ14	CCCAAGCTTAACGAGATGGCAACAGCA (HindIII)	
LXR101A	GTCTCGTACGAAGAGCTTTTATAAAAGCTTGATCGCCGAGAACCCCTG	
LXR101B	AAAATCCCTTAACGTGAGCCTAGGGCGTGCAACGAGATGGCAACAGCA	
WQ15	CCTGCAAGGCCTGTTCGG	Confirmation of *hspR* deletion in Δ*hspR* strain
WQ16	AGGGCTATGACGGTACGA	
WQ17	ACCGTCTCGGCCTGGTCT	
WQ18	CTCGCGCTGCTGCATCAT	
LXR133A	CCGGAATTCGATGGCGTCCTCGTGCTC (EcoRI)	Complementation of *hspR* in Δ*hspR* strain
LXR133B	CGGGATCCTTCAATTCCTCCAGCAA (BamHI)	
LXR134A	CGGGATCCGAGGAGATGGACGGCCGT (BamHI)	
LXR134B	CCCAAGCTTCGAAGCCGTCAGTCCGAG (HindIII)	
WQ25	CGGGATCCCCGCGAAGGGAGCATGAGG (BamHI)	Overexpression of *hspR* in *Streptomyces*
WQ26	CCCAAGCTTCTGGACAGTCTCGGTGCCG (HindIII)	
WQ27	CCGGAATTCCATGAGGAGATGGACGGC (EcoRI)	Expression of His_6-HspR protein in *E. coli*
WQ28	CCCAAGCTTACATGCTGGACAGTCTCG (HindIII)	
LXR60A	CCCAAGCTTGGAGGTGGCATGGACTAC (HindIII)	Amplification of 3×FLAG fragment
LXR60B	CGGGATCCTCCGGTTGACCCTTATTT (BamHI)	
LXR136A	GCTCTAGAGATGGCGTCCTCGTGCTC (XbaI)	Complementation of *hspR* in Δ*hspR* strain with 3×FLAG-tagged HspR
LXR136B	TTCAATTCCTCCAGCAA	
LXR135A	TCATTGCTGGAGGAATTGAAGAGGAGATGGACGGCCGT	
LXR135B	CCCAAGCTTGTCCGAGGACTGGCGCTT (HindIII)	
EMSA		
aveA1p-Fw	ATGGTCGGGAACCTCCGCAA	Probe *aveA1p*
aveA1p-Rev	CTGTGTCCTCACCGCTAGGC	
LXR59A	ATCTAGTCGTTTTTGAGT	Probe *hrdBp*
LXR59B	ACGAACAACCTCTCGGAA	
aveA4p-Fw	CGACAAGAGAAATCGGAAATT	Probe *aveA4p*
aveA4p-Rev	GCCTGCACCTGTGACAAG	
aveRp-Fw	CCGCACCGCCATACATAC	Probe *aveRp*
aveRp-Rev	GAAACTCCCTGCATGATGTTC	
LXR102A	GGGCATCAATGTCTTGAACGTCTTCAACTCTTCAAAGCTAATGACGGCGC	Probe *aveA1p*-1
LXR102B	GCGCCGTCATTAGCTTTGAAGAGTTGAAGACGTTCAAGACATTGATGCCC	
LXR103A	GGGCATCAATGTCAAGCTTGTCTTCAGGATCCCAAAGCTAATGACGGCGC	Probe *aveA1p*-1m
LXR103B	GCGCCGTCATTAGCTTTGGGATCCTGAAGACAAGCTTGACATTGATGCCC	
WQ39	AGGAGCGGATAAGACTTGAGT	Probe *dnaK1p*
WQ40	TTAGTCGTGCCCAGGTCG	
LXR104A	TAAGGAGCGGATAAGACTTGAGTCGGCTCGACTCAGGTCTGTTGACCCAG	Probe *dnaK1p*-1
LXR104B	CTGGGTCAACAGACCTGAGTCGAGCCGACTCAAGTCTTATCCGCTCCTTA	
LXR105A	TAAGGAGCGGATAAGACAAGCTTCGGCTCGGGATCCGTCTGTTGACCCAG	Probe *dnaK1p*-1m
LXR105B	CTGGGTCAACAGACGGATCCCGAGCCGAAGCTTGTCTTATCCGCTCCTTA	

(Continued on next page)

TABLE 2 (Continued)

Primer	DNA sequence[a] (5′→3′)	Use
LXR106A	TTGGGTGATGCACACTTGAGTCCGTTCCACTCAAGTCATTGCTGGAGGAA	Probe *dnaK1p*-2
LXR106B	TTCCTCCAGCAATGACTTGAGTGGAACGGACTCAAGTGTGCATCACCCAA	
LXR107A	TTGGGTGATGCACACAAGCTTCCGTTCCGGATCCGTCATTGCTGGAGGAA	Probe *dnaK1p*-2m
LXR107B	TTCCTCCAGCAATGACGGATCCGGAACGGAAGCTTGTGTGCATCACCCAA	
LXR108A	CATGGGGCCGAACCTAGC	Probe *clpB1p*
LXR108B	TCGCTGTCTCCTCCTGTG	
LXR109A	AAGGAAGAGGCGGGCGTG	Probe *clpB2p*
LXR109B	CGACCGGATCCGACGCG	
LXR110A	GAAGCACCTGGTTCGCCT	Probe *lonAp*
LXR110B	AAGCCATGATCTCCCCTT	
SD335A	CGTTCTCCTCGAGCCTACAGG	Probe *dnaK2p*
SD335B	CTCCCACACGGCGATCAC	
SD339A	ATTGGCACTCCGCTTGAC	Probe *groES1p*
SD339B	GGCTTGATGGCAACCTTG	
SD337A	TTCAGATGGACGGCTACC	Probe *groEL2p*
SD337B	AGAGTGCTAACGCCAATGA	
SD340A	GGAAAGCCGCTGGTCAGAC	Probe *htpGp*
SD340B	GGGAGTCCATCGTCGCAG	
SD341A	ATCGTCCCTGGTCATCGG	Probe *hsp18_1p*
SD341B	ATCAACATCGTGAAACACCTCC	
SD342A	AGTGCTGTCGTCGCTCAT	Probe *hsp18_2p*
SD342B	CATCAACACGGTAAACACCTC	
SD123A	GCGCAGTCGTTCCAGTAG	Probe *catR_katA1*
SD123B	GGACTCGCTGTTCTGATTGT	
SD124A	GGAAAGGTGGTCTGGTTC	Probe *katA2p*
SD124B	GGTGTACGGAGCCTTCTG	
SD122A	AGGTCCGTGGAGCGCCTC	Probe *katA3p*
SD122B	CGGTGGCTGAGTTCTGGTTGTC	
SD236A	GAGAAGCCGAGCACCTGG	Probe *oxyR_ahpCD*
SD236B	CGCTGGAGAAGGGCAATG	
SD210A	CCGATGGCTGTAGGCGTTTAT	Probe *whiBp*
SD210B	CCCTCGTCTGTCTTCGCG	
LXR111A	GAGCGCGTTTTCTCCGAG	Probe *ssgYp*
LXR111B	ATGCAGCCCCTGAATTTC	
LXR112A	ATCTTCGGCACTCTACGT	Probe *wblBp*
LXR112B	AAATCTGCCATTACGTGT	
SD115A	GCCCGGTTCTCGTAAGAC	Probe *ftsHp*
SD115B	CAGCACGATCCACATGAC	
DNase I footprinting		
FAM-WQ45	CCCAGCGCACGATTCATGA	*aveA1* promoter region
WQ46	CCGTCCATCCTCTGCACCTG	
FAM-WQ43	GTCTCGGTCCTCGGGCTG	*dnaK1* promoter region
WQ44	TGCTGCGGGTTGAAGTCC	
RT-qPCR		
16S-QP-Fw	AGCGGAGCATGTGGCTTAAT	16S rRNA ORF
16S-QP-Rev	ACGTATTCACCGCAGCAATG	

(Continued on next page)

TABLE 2 (Continued)

Primer	DNA sequence[a] (5′→3′)	Use
GJ99	CGGACAGGACTACGCACTTC	*aveA1* ORF
GJ100	ACGAGATACGACCGGAGATC	
LXR32A	ATCTCGTCAAGTCCCAGA	*aveA2* ORF
LXR32B	GTGTAACTGGTTCCTGAG	
SD346A	CCAAGAACGGTGAGGTGC	*dnaK1* ORF
SD346B	CTGCTGCGGGTTGAAGTC	
LXR113A	TCGGAACCCCTATGAACT	*hspR* ORF
LXR113B	GTACTGACGCAGGGTCTG	
LXR114A	CCTCAAGAACAAGCGGCT	*clpB1* ORF
LXR114B	CGGCGAGCACGGTCTTCA	
LXR115A	ATGAACCGTCTCACCCAG	*clpB2* ORF
LXR115B	TCCTCCTGATCGAGAAGT	
LXR116A	AAGGGGAGATCATGGCTT	*lonA* ORF
LXR116B	GGCGTCGTTCAGGTCCAG	
katA1-QP-Fw	ACCTCGTCGGCAACAACAC	*katA1* ORF
katA1-QP-Rev	TGTACGGGTCGCGCTTCTG	
catR-QP-Fw	TGAAGCTGCCCGAGATCTCC	*catR* ORF
catR-QP-Rev	CTTGTCCGTGGCGACCTCC	
katA3-QP-Fw	CATCCACTCCCAGAAGCGC	*katA3* ORF
katA3-QP-Rev	TCGCCCATCAGCCAGGTC	
oxyR-QP-Fw	GATGGAGGAGGCCGAGGC	*oxyR* ORF
oxyR-QP-Rev	GCAGGAGGTTGAGCTCACG	
ahpC-QP-Fw	CCAGGTGCTCGGCTTCTCC	*ahpC* ORF
ahpC-QP-Rev	GAAGCACGAGCTGATGCGC	
ahpD-QP-Fw	CTCTCGATGAACTGAAGG	*ahpD* ORF
ahpD-QP-Rev	TGCGGCAGGTCGGAGTTG	
LXR117A	TCACAGTCATCCCAGGCAT	*htpG* ORF
LXR117B	CTCGCGCAGATAGACCTT	
LXR118A	CGATGCCAATGGACGCCTA	*hsp18_1* ORF
LXR118B	TCAGCATGTTCCGTTCGA	
LXR119A	ATCTGATGGGTCCGGGAA	*hsp18_2* ORF
LXR119B	AAGGCGATGACGTACTGG	
LXR120A	CAGCTCGCTCTTCTTCCA	*wblB* ORF
LXR120B	TCATGCAGACCTCTTTGG	
LXR121A	AATGGATCATCGGACGAGA	*ssgY* ORF
LXR121B	TGTACGAGTCGGAGCGGTCAG	
SD247A	CGGCTACAAGACAGTGGACA	*ftsH* ORF
SD247B	GACCTTGATGACCTGCTCGT	
LXR122A	GCACCGTCCAGCAGTTGT	*hspR* deletion region
LXR122B	ACTCCAGTTCCACCACGC	
ChIP-qPCR		
LXR123A	AGGGGTGGATAGGGGTATT	*aveA1* promoter DNA
LXR123B	AAGAATGAAAGGAGCGCG	
LXR69A	CACTCGTGAATTGTGGAC	*aveR* promoter DNA
LXR69B	TGACTTTGATGATTAACT	

(Continued on next page)

TABLE 2 (Continued)

Primer	DNA sequence[a] (5′→3′)	Use
LXR124A	CGTGTAAGGAGCGGATAA	*dnaK1* promoter DNA
LXR124B	TTCAATTCCTCCAGCAAT	
LXR125A	TTCCCGGCACCCCCGAA	*clpB1* promoter DNA
LXR125B	TCTGACATTGGAAGCGTA	
LXR126A	ACGAGCGGCGGTGGCGGT	*clpB2* promoter DNA
LXR126B	CGACCGGATCCGACGCG	
LXR127A	ATTTCCGATGATCGCTGA	*lonA* promoter DNA
LXR127B	AAGCCATGATCTCCCCTT	
LXR128A	TGTGACTTTGGAGCTTTA	*catR_katA1* promoter DNA
LXR128B	TCCTGCGTCATTCCTGCAA	
LXR129A	GGAACCAACTTCAACAAA	*katA3* promoter DNA
LXR129B	TTCGACATCGTGCACCTT	
LXR130A	AAGATGACCTTCCACTGA	*oxyR_ahpC* promoter DNA
LXR130B	TGACAAGTTCCCCGAGTT	
LXR131A	TTCGTCACCCTGGGGGTG	*dnaK2* promoter DNA
LXR131B	ACTCTCCGGATCACGTTC	
LXR132A	CCCAGAACCGAACCGAAG	*katA2* promoter DNA
LXR132B	AAAGAAGAGGGTCGTTAG	

[a]Underlining indicates sequences for the restriction enzymes shown in parentheses.

Scanning electron microscopy. Mycelia and spores of *S. avermitilis* WT and Δ*hspR* grown on YMS plates for 2 or 4 days were observed by SEM. Samples were prepared and examined as described in our previous study (51).

Production and analysis of avermectins. Avermectin yield from *S. avermitilis* fermentation culture was analyzed by HPLC as described previously (52).

Heterologous expression and purification of His_6-HspR. For expression of *S. avermitilis* HspR in *E. coli*, the 579-bp *hspR* ORF was generated by PCR using primers WQ27 and WQ28. The PCR fragment was digested with EcoRI/XhoI and ligated into pET-28a(+), generating pET28-*hspR* for overexpression of N-terminal His_6-tagged HspR recombinant protein. Expression vector pET28-*hspR* was confirmed by sequencing and transformed into *E. coli* BL21(DE3). His_6-HspR expression was induced by 3-h treatment with 0.2 mM isopropyl-β-D-thiogalactopyranoside (IPTG) at 37°C. Cell lysates were prepared by sonication on ice in lysis buffer (53) and centrifugation. Soluble His_6-HspR was purified on an Ni-nitrilotriacetic acid (NTA) column (Bio-Works; Sweden) and eluted by lysis buffer with 250 mM imidazole. The purified protein was dialyzed in binding buffer for EMSAs (54) to eliminate imidazole and stored at −80°C until use.

Electrophoretic mobility shift assays. Promoter probes of tested genes were amplified by PCR with corresponding primers listed in Table 2, and labeled at the 3′ end with nonradioactive digoxigenin-1-ddUTP. EMSAs were performed as described previously (52). Specificity of the HspR-probe interaction was tested by adding ~300-fold excess of unlabeled nonspecific probe (*hrdBp*) or respective specific probe to the binding reaction system.

Reverse transcription and real-time quantitative PCR analysis. Total RNAs were extracted from *S. avermitilis* cultures grown in FM-I or FM-II or on YMS plates for various durations. RNA isolation, removal of genomic DNA, and subsequent RT-qPCR analysis (using primers listed in Table 2) were performed as described previously (52). Relative expression levels of tested genes were normalized with 16S rRNA (housekeeping gene) as the internal control. Experiments were performed in triplicates.

Western blotting. Total protein was prepared at various time points from Δ*hspR*/*hspR*-3FLAG mycelia grown in FM-I. Western blotting was performed as described in our previous study (54), using 1:3,300-diluted mouse anti-FLAG monoclonal antibody (MAb) (Sigma; USA).

ChIP-qPCR. To prepare samples for ChIP-qPCR, *S. avermitilis* WT, WT/*hspR*-3FLAG, Δ*hspR*/*hspR*-3FLAG, and Δ*phoP*/*hspR*-3FLAG strains were cultured in FM-II, and mycelia were harvested at various time points and treated as described previously (29). Immunoprecipitation reactions and ChIP-qPCR data analysis were performed as described previously (32, 48). Relative protein enrichment of each site was normalized based on input chromosomal DNA, and binding level was shown as a percentage of input DNA. Experiments were performed in triplicates.

DNase I footprinting. To determine HspR binding sites, 5′ 6-carboxyfluorescein (FAM)-labeled DNA fragments corresponding to *aveA1* and *dnaK1* promoter regions were PCR-synthesized using primers listed in Table 2 and then purified. DNase I footprinting assays were performed as described previously (51, 55), and data were analyzed using GeneMarker software program v2.2.0.

GST pulldown. pET28-hspR (for His_6-HspR expression) and pGEX-PhoP (for GST-PhoP expression) (38) were cotransformed into *E. coli* BL21(DE3). Bacteria containing pET28-hspR and pGEX-4T-1 (for GST tag expression) were used as negative controls. Following 0.4 mM IPTG induction for 3 h at 37°C, cells containing both His_6- and GST-tagged proteins were sonicated in lysis buffer (53) on ice and centrifuged. One milliliter cell lysate and 50 μl 50% glutathione-Sepharose beads (equilibrated with lysis buffer) were incubated overnight at 4°C. Beads were washed four times with phosphate-buffered saline (PBS) (56), and the resulting pellet was boiled with 50 μl protein loading buffer. Eluted bound proteins were separated by electrophoresis on SDS-PAGE gels and identified by Western blotting using anti-His_6 or anti-GST antibody (Tiangen; China).

SUPPLEMENTAL MATERIAL

Supplemental material is available online only.

SUPPLEMENTAL FILE 1, PDF file, 0.7 MB.

ACKNOWLEDGMENTS

This study was supported by the National Natural Science Foundation of China (grant 31872629) and the Project for Extramural Scientists of the State Key Laboratory of Agrobiotechnology (grant 2020SKLAB6-4).

We thank S. Anderson for English editing of the manuscript.

REFERENCES

1. Flardh K, Buttner MJ. 2009. *Streptomyces* morphogenetics: dissecting differentiation in a filamentous bacterium. Nat Rev Microbiol 7:36–49. https://doi.org/10.1038/nrmicro1968.
2. Demain AL. 2002. Prescription for an ailing pharmaceutical industry. Nat Biotechnol 20:331. https://doi.org/10.1038/nbt0402-331.
3. Challis GL, Hopwood DA. 2003. Synergy and contingency as driving forces for the evolution of multiple secondary metabolite production by *Streptomyces* species. Proc Natl Acad Sci U S A 100(Suppl 2):14555–14561. https://doi.org/10.1073/pnas.1934677100.
4. Bibb MJ. 2005. Regulation of secondary metabolism in streptomycetes. Curr Opin Microbiol 8:208–215. https://doi.org/10.1016/j.mib.2005.02.016.
5. Liu G, Chater KF, Chandra G, Niu G, Tan H. 2013. Molecular regulation of antibiotic biosynthesis in *Streptomyces*. Microbiol Mol Biol Rev 77:112–143. https://doi.org/10.1128/MMBR.00054-12.
6. Yoon V, Nodwell JR. 2014. Activating secondary metabolism with stress and chemicals. J Ind Microbiol Biotechnol 41:415–424. https://doi.org/10.1007/s10295-013-1387-y.

7. Georgopoulos C, Welch WJ. 1993. Role of the major heat shock proteins as molecular chaperones. Annu Rev Cell Biol 9:601–634. https://doi.org/10.1146/annurev.cb.09.110193.003125.
8. Gottesman S, Wickner S, Maurizi MR. 1997. Protein quality control: triage by chaperones and proteases. Genes Dev 11:815–823. https://doi.org/10.1101/gad.11.7.815.
9. Hendrick JP, Hartl FU. 1993. Molecular chaperone functions of heat-shock proteins. Annu Rev Biochem 62:349–384. https://doi.org/10.1146/annurev.bi.62.070193.002025.
10. Schumann W. 2016. Regulation of bacterial heat shock stimulons. Cell Stress Chaperones 21:959–968. https://doi.org/10.1007/s12192-016-0727-z.
11. Grandvalet C, Rapoport G, Mazodier P. 1998. *hrcA*, encoding the repressor of the *groEL* genes in *Streptomyces albus* G, is associated with a second *dnaJ* gene. J Bacteriol 180:5129–5134. https://doi.org/10.1128/JB.180.19.5129-5134.1998.
12. Servant P, Grandvalet C, Mazodier P. 2000. The RheA repressor is the thermosensor of the HSP18 heat shock response in *Streptomyces albus*. Proc Natl Acad Sci U S A 97:3538–3543. https://doi.org/10.1073/pnas.070426197.
13. Bucca G, Hindle Z, Smith CP. 1997. Regulation of the *dnaK* operon of *Streptomyces coelicolor* A3(2) is governed by HspR, an autoregulatory repressor protein. J Bacteriol 179:5999–6004. https://doi.org/10.1128/jb.179.19.5999-6004.1997.
14. Bucca G, Brassington AM, Hotchkiss G, Mersinias V, Smith CP. 2003. Negative feedback regulation of *dnaK*, *clpB* and *lon* expression by the DnaK chaperone machine in *Streptomyces coelicolor*, identified by transcriptome and *in vivo* DnaK-depletion analysis. Mol Microbiol 50:153–166. https://doi.org/10.1046/j.1365-2958.2003.03696.x.
15. Grandvalet C, Servant P, Mazodier P. 1997. Disruption of *hspR*, the repressor gene of the *dnaK* operon in *Streptomyces albus* G. Mol Microbiol 23:77–84. https://doi.org/10.1046/j.1365-2958.1997.1811563.x.
16. Grandvalet C, de Crecy-Lagard V, Mazodier P. 1999. The ClpB ATPase of *Streptomyces albus* G belongs to the HspR heat shock regulon. Mol Microbiol 31:521–532. https://doi.org/10.1046/j.1365-2958.1999.01193.x.
17. Sobczyk A, Bellier A, Viala J, Mazodier P. 2002. The *lon* gene, encoding an ATP-dependent protease, is a novel member of the HAIR/HspR stress-response regulon in actinomycetes. Microbiology (Reading) 148:1931–1937. https://doi.org/10.1099/00221287-148-6-1931.
18. Bucca G, Brassington AM, Schonfeld HJ, Smith CP. 2000. The HspR regulon of *Streptomyces coelicolor*: a role for the DnaK chaperone as a transcriptional co-repressor. Mol Microbiol 38:1093–1103. https://doi.org/10.1046/j.1365-2958.2000.02194.x.
19. Stewart GR, Wernisch L, Stabler R, Mangan JA, Hinds J, Laing KG, Young DB, Butcher PD. 2002. Dissection of the heat-shock response in *Mycobacterium tuberculosis* using mutants and microarrays. Microbiology (Reading) 148:3129–3138. https://doi.org/10.1099/00221287-148-10-3129.
20. Singh R, Anil Kumar V, Das AK, Bansal R, Sarkar D. 2014. A transcriptional co-repressor regulatory circuit controlling the heat-shock response of *Mycobacterium tuberculosis*. Mol Microbiol 94:450–465. https://doi.org/10.1111/mmi.12778.
21. Martin JF. 2004. Phosphate control of the biosynthesis of antibiotics and other secondary metabolites is mediated by the PhoR-PhoP system: an unfinished story. J Bacteriol 186:5197–5201. https://doi.org/10.1128/JB.186.16.5197-5201.2004.
22. Martin JF, Santos-Beneit F, Rodriguez-Garcia A, Sola-Landa A, Smith MCM, Ellingsen TE, Nieselt K, Burroughs NJ, Wellington EMH. 2012. Transcriptomic studies of phosphate control of primary and secondary metabolism in *Streptomyces coelicolor*. Appl Microbiol Biotechnol 95:61–75. https://doi.org/10.1007/s00253-012-4129-6.
23. Martin JF, Rodriguez-Garcia A, Liras P. 2017. The master regulator PhoP coordinates phosphate and nitrogen metabolism, respiration, cell differentiation and antibiotic biosynthesis: comparison in *Streptomyces coelicolor* and *Streptomyces avermitilis*. J Antibiot 70:534–541. https://doi.org/10.1038/ja.2017.19.
24. Allenby NEE, Laing E, Bucca G, Kierzek AM, Smith CP. 2012. Diverse control of metabolism and other cellular processes in *Streptomyces coelicolor* by the PhoP transcription factor: genome-wide identification of in vivo targets. Nucleic Acids Res 40:9543–9556. https://doi.org/10.1093/nar/gks766.
25. Sola-Landa A, Rodriguez-Garcia A, Amin R, Wohlleben W, Martin JF. 2013. Competition between the GlnR and PhoP regulators for the *glnA* and *amtB* promoters in *Streptomyces coelicolor*. Nucleic Acids Res 41:1767–1782. https://doi.org/10.1093/nar/gks1203.
26. Santos-Beneit F, Rodriguez-Garcia A, Sola-Landa A, Martin JF. 2009. Cross-talk between two global regulators in *Streptomyces*: PhoP and AfsR interact in the control of *afsS*, *pstS* and *phoRP* transcription. Mol Microbiol 72:53–68. https://doi.org/10.1111/j.1365-2958.2009.06624.x.
27. Burg RW, Miller BM, Baker EE, Birnbaum J, Currie SA, Hartman R, Kong YL, Monaghan RL, Olson G, Putter I, Tunac JB, Wallick H, Stapley EO, Oiwa R, Omura S. 1979. Avermectins, new family of potent anthelmintic agents: producing organism and fermentation. Antimicrob Agents Chemother 15:361–367. https://doi.org/10.1128/AAC.15.3.361.
28. Egerton JR, Ostlind DA, Blair LS, Eary CH, Suhayda D, Cifelli S, Riek RF, Campbell WC. 1979. Avermectins, new family of potent anthelmintic agents: efficacy of the B1a component. Antimicrob Agents Chemother 15:372–378. https://doi.org/10.1128/AAC.15.3.372.
29. Guo J, Zhao J, Li L, Chen Z, Wen Y, Li J. 2010. The pathway-specific regulator AveR from *Streptomyces avermitilis* positively regulates avermectin production while it negatively affects oligomycin biosynthesis. Mol Genet Genomics 283:123–133. https://doi.org/10.1007/s00438-009-0502-2.
30. Kitani S, Ikeda H, Sakamoto T, Noguchi S, Nihira T. 2009. Characterization of a regulatory gene, *aveR*, for the biosynthesis of avermectin in *Streptomyces avermitilis*. Appl Microbiol Biotechnol 82:1089–1096. https://doi.org/10.1007/s00253-008-1850-2.
31. Ikeda H, Nonomiya T, Usami M, Ohta T, Omura S. 1999. Organization of the biosynthetic gene cluster for the polyketide anthelmintic macrolide avermectin in *Streptomyces avermitilis*. Proc Natl Acad Sci U S A 96:9509–9514. https://doi.org/10.1073/pnas.96.17.9509.
32. Lu X, Liu X, Chen Z, Li J, van Wezel GP, Chen W, Wen Y. 2020. The ROK-family regulator Rok7B7 directly controls carbon catabolite repression, antibiotic biosynthesis, and morphological development in *Streptomyces avermitilis*. Environ Microbiol 22:5090–5108. https://doi.org/10.1111/1462-2920.15094.
33. Tanaka A, Takano Y, Ohnishi Y, Horinouchi S. 2007. AfsR recruits RNA polymerase to the *afsS* promoter: a model for transcriptional activation by SARPs. J Mol Biol 369:322–333. https://doi.org/10.1016/j.jmb.2007.02.096.
34. Yin S, Wang W, Wang X, Zhu Y, Jia X, Li S, Yuan F, Zhang Y, Yang K. 2015. Identification of a cluster-situated activator of oxytetracycline biosynthesis and manipulation of its expression for improved oxytetracycline production in *Streptomyces rimosus*. Microb Cell Fact 14:46. https://doi.org/10.1186/s12934-015-0231-7.
35. Sun D, Wang Q, Chen Z, Li J, Wen Y. 2017. An alternative sigma factor, σ^8, controls avermectin production and multiple stress responses in *Streptomyces avermitilis*. Front Microbiol 8:736. https://doi.org/10.3389/fmicb.2017.00736.
36. Liu X, Sun M, Cheng Y, Yang R, Wen Y, Chen Z, Li J. 2016. OxyR is a key regulator in response to oxidative stress in *Streptomyces avermitilis*. Microbiology (Reading) 162:707–716. https://doi.org/10.1099/mic.0.000251.
37. Sola-Landa A, Rodriguez-Garcia A, Franco-Dominguez E, Martin JF. 2005. Binding of PhoP to promoters of phosphate-regulated genes in *Streptomyces coelicolor*: identification of PHO boxes. Mol Microbiol 56:1373–1385. https://doi.org/10.1111/j.1365-2958.2005.04631.x.
38. Yang R, Liu X, Wen Y, Song Y, Chen Z, Li J. 2015. The PhoP transcription factor negatively regulates avermectin biosynthesis in *Streptomyces avermitilis*. Appl Microbiol Biotechnol 99:10547–10557. https://doi.org/10.1007/s00253-015-6921-6.
39. Hiard S, Maree R, Colson S, Hoskisson PA, Titgemeyer F, van Wezel GP, Joris B, Wehenkel L, Rigali S. 2007. PREDetector: a new tool to identify regulatory elements in bacterial genomes. Biochem Biophys Res Commun 357:861–864. https://doi.org/10.1016/j.bbrc.2007.03.180.
40. Bush MJ, Chandra G, Bibb MJ, Findlay KC, Buttner MJ. 2016. Genome-wide chromatin immunoprecipitation sequencing analysis shows that WhiB is a transcription factor that cocontrols its regulon with WhiA to initiate developmental cell division in *Streptomyces*. mBio 7:e00523-16. https://doi.org/10.1128/mBio.00523-16.
41. Molle V, Palframan WJ, Findlay KC, Buttner MJ. 2000. WhiD and WhiB, homologous proteins required for different stages of sporulation in *Streptomyces coelicolor* A3(2). J Bacteriol 182:1286–1295. https://doi.org/10.1128/JB.182.5.1286-1295.2000.
42. Willemse J, Borst JW, de Waal E, Bisseling T, van Wezel GP. 2011. Positive control of cell division: FtsZ is recruited by SsgB during sporulation of *Streptomyces*. Genes Dev 25:89–99. https://doi.org/10.1101/gad.600211.
43. Liu W, Zhang Q, Guo J, Chen Z, Li J, Wen Y. 2015. Increasing avermectin production in *Streptomyces avermitilis* by manipulating the expression of a novel TetR-family regulator and its target gene product. Appl Environ Microbiol 81:5157–5173. https://doi.org/10.1128/AEM.00868-15.
44. Ikeda H, Kotaki H, Tanaka H, Omura S. 1988. Involvement of glucose catabolism in avermectin production by *Streptomyces avermitilis*. Antimicrob Agents Chemother 32:282–284. https://doi.org/10.1128/AAC.32.2.282.

45. Jiang L, Liu Y, Wang P, Wen Y, Song Y, Chen Z, Li J. 2011. Inactivation of the extracytoplasmic function sigma factor Sig6 stimulates avermectin production in *Streptomyces avermitilis*. Biotechnol Lett 33:1955–1961. https://doi.org/10.1007/s10529-011-0673-x.
46. Bierman M, Logan R, O'Brien K, Seno ET, Rao RN, Schoner BE. 1992. Plasmid cloning vectors for the conjugal transfer of DNA from *Escherichia coli* to *Streptomyces* spp. Gene 116:43–49. https://doi.org/10.1016/0378-1119(92)90627-2.
47. Li P, Li J, Guo Z, Tang W, Han J, Meng X, Hao T, Zhu Y, Zhang L, Chen Y. 2015. An efficient blue-white screening based gene inactivation system for *Streptomyces*. Appl Microbiol Biotechnol 99:1923–1933. https://doi.org/10.1007/s00253-014-6369-0.
48. Yan H, Lu X, Sun D, Zhuang S, Chen Q, Chen Z, Li J, Wen Y. 2020. BldD, a master developmental repressor, activates antibiotic production in two *Streptomyces* species. Mol Microbiol 113:123–142. https://doi.org/10.1111/mmi.14405.
49. Li L, Guo J, Wen Y, Chen Z, Song Y, Li J. 2010. Overexpression of ribosome recycling factor causes increased production of avermectin in *Streptomyces avermitilis* strains. J Ind Microbiol Biotechnol 37:673–679. https://doi.org/10.1007/s10295-010-0710-0.
50. Pullan ST, Chandra G, Bibb MJ, Merrick M. 2011. Genome-wide analysis of the role of GlnR in *Streptomyces venezuelae* provides new insights into global nitrogen regulation in actinomycetes. BMC Genomics 12:175. https://doi.org/10.1186/1471-2164-12-175.
51. Sun D, Zhu J, Chen Z, Li J, Wen Y. 2016. SAV742, a novel AraC-family regulator from *Streptomyces avermitilis*, controls avermectin biosynthesis, cell growth and development. Sci Rep 6:36915. https://doi.org/10.1038/srep36915.
52. Luo S, Sun D, Zhu J, Chen Z, Wen Y, Li J. 2014. An extracytoplasmic function sigma factor, σ^{25}, differentially regulates avermectin and oligomycin biosynthesis in *Streptomyces avermitilis*. Appl Microbiol Biotechnol 98:7097–7112. https://doi.org/10.1007/s00253-014-5759-7.
53. Guo J, Zhang X, Lu X, Liu W, Chen Z, Li J, Deng L, Wen Y. 2018. SAV4189, a MarR-family regulator in *Streptomyces avermitilis*, activates avermectin biosynthesis. Front Microbiol 9:1358. https://doi.org/10.3389/fmicb.2018.01358.
54. Zhu J, Sun D, Liu W, Chen Z, Li J, Wen Y. 2016. AvaR2, a pseudo gamma-butyrolactone receptor homologue from *Streptomyces avermitilis*, is a pleiotropic repressor of avermectin and avenolide biosynthesis and cell growth. Mol Microbiol 102:562–578. https://doi.org/10.1111/mmi.13479.
55. Zianni M, Tessanne K, Merighi M, Laguna R, Tabita FR. 2006. Identification of the DNA bases of a DNase I footprint by the use of dye primer sequencing on an automated capillary DNA analysis instrument. J Biomol Tech 17:103–113.
56. Zhu J, Chen Z, Li J, Wen Y. 2017. AvaR1, a butenolide-type autoregulator receptor in *Streptomyces avermitilis*, directly represses avenolide and avermectin biosynthesis and multiple physiological responses. Front Microbiol 8:2577. https://doi.org/10.3389/fmicb.2017.02577.